Journal of Medicinal Chemistry

Freie Universität Berlin

Article

Structure Activity Relationship, Drug Metabolism and Pharmacokinetics Properties Optimization and In Vivo Studies of New Brain Penetrant Triple T-Type Calcium Channel Blockers

Romain Siegrist, Davide Pozzi, Gaël Jacob, Caterina Torrisi, Kilian Colas, Bertrand Braibant, Jacques Mawet, Thomas Pfeifer, Ruben de Kanter, Catherine Roch, Melanie Kessler, Olivier Corminboeuf, and Olivier Bezençon

J. Med. Chem., **Just Accepted Manuscript** • DOI: 10.1021/acs.jmedchem.6b01356 • Publication Date (Web): 04 Nov 2016

ACS Publications

Journal of Medicinal Chemistry is published by the American Chemical Society. 1155 Sixteenth Street N.W., Washington, DC 20036

Structure Activity Relationship, Drug Metabolism and Pharmacokinetics Properties Optimization and *In Vivo* Studies of New Brain Penetrant Triple T-Type Calcium Channel Blockers

*Romain Siegrist‡, Davide Pozzi‡, Gaël Jacob, Caterina Torrisi, Kilian Colas, Bertrand Braibant, Jacques Mawet, Thomas Pfeifer†, Ruben de Kanter, Catherine Roch, Melanie Kessler, Olivier Corminboeuf and Olivier Bezençon**

Drug Discovery Chemistry, Biology and Pharmacology, Actelion Pharmaceuticals Ltd., Gewerbestrasse 16, CH-4123 Allschwil, Switzerland.

T-type calcium channel, Ca_v 3.1, Ca_v 3.2, Ca_v 3.3, 1,4-benzodiazepines, epilepsy.

ABSTRACT

Despite the availability of numerous antiepileptic drugs, 20-30% of epileptic patients are pharmacoresistant with seizures not appropriately controlled. Consequently, new strategies to address this unmet medical need are required. T-type calcium channels play a key role in neuronal excitability and burst firing and selective triple T-type calcium channel blockers could offer a new way to treat various CNS disorders, in particular epilepsy. Herein we describe the identification of new 1,4-benzodiazepines as brain penetrant and selective triple T-type calcium channel blockers. From racemic hit **4**, optimization work led to the preparation of pyridodiazepine **31c** with improved physicochemical properties, solubility and metabolic

stability. The racemic mixture was separated by chiral preparative HPLC and the resulting lead compound **(3*R*,5*S*)-31c** showed promising efficacy in the WAG/Rij-rat model of generalized non-convulsive absence-like epilepsy.

INTRODUCTION

Epilepsy affects more than fifty million people worldwide. This chronic neurological disorder of the brain is characterized by an enduring predisposition to generate seizures. More than forty different epilepsy syndromes, defined by seizure types and other clinical features, are reported. Around twenty-eight antiepileptic drugs (AEDs) are available to patients, many of which modulate excitatory or inhibitory synaptic activity and have multiple targets. Despite the plethora of AEDs available and their use in combination therapy, 20-30% of the epileptic patients are unable to achieve seizure freedom. Clinical and experimental data indicate that drug-resistance might arise from alterations of drug targets or augmentation of multidrug transporter function[1]. Furthermore, most AEDs present significant side effects such as sedation, cognitive dysfunctions, weight disorder, or teratogenic potential. Therefore, newer, safer, and more efficient medications are necessary to treat this unmet medical need[2-3].

Calcium channels control many important physiological processes. They allow the influx of calcium into the cytosol, which lead to the modulation of several cellular processes, like neuronal excitability, neurotransmitters and hormones release, pain sensation, muscle contractions, or cell development and proliferation. Both ligand-bound or voltage-gated calcium channels are known. Voltage-gated channels can be further classified in high- (HVA) or low-voltage-activated (LVA) calcium channels. HVA calcium channels are subdivided in L-, N-, P-/Q-, or R-types based on their α-subunits. LVA calcium channels, also referred to as T-type (T for transient) calcium

channels, are subcategorized in $Ca_V3.1$ (α1G), $Ca_V3.2$ (α1H), and $Ca_V3.3$(α1I). Physiologically, calcium T-channels are involved in the regulation of membrane potential and in the control of intracellular calcium concentration[4]. In the brain, the three T-type calcium channel subtypes are widely expressed[5] and play a key role in the regulation of neuronal excitability and network oscillation activities[6, 7].

Inhibition of the T-type calcium channels could be useful for the treatment of several central[8] or peripheral diseases like Parkinson's disease[9], pain[10], oncology[11], sleep disorders[12], or epilepsy[13-15] and could also play a role in neuroprotection[16]. Strong evidences link T-type calcium channels with epilepsy. Pharmacological studies using genetic models of generalized non-convulsive absence-like epilepsy (the generalized absence epilepsy rat of Strasbourg,GAERS or the WAG/Rij (Wistar Albino Glaxo from Rijswijk-rat) showed that T-type calcium channel blockers strongly decreased the epileptic activity in those models[17, 18]. In addition, mice overexpressing the $Ca_V3.1$ channels present frequent spike wave discharges (the hallmark of absence seizures)[19] whereas, knockout mice lacking the $Ca_V3.1$ gene are protected from absence seizures[20]. Finally, mutations in CACNA1H, the gene encoding the $Ca_V3.2$ channel, have been found in patients suffering from idiopathic generalized epilepsy[21].

Despite the attractive therapeutic potential, more than twenty years were necessary to overcome the poor specificity of the antihypertensive drug mibefradil, a T- and L-type calcium channel blocker, and to discover the first selective T-type calcium channel blocker[22]. Since then, several chemically diverse selective triple T-type calcium channel blockers (blocking the 3 subtypes) have been reported[23, 24] and at least three of them have reached clinical trials (Figure 1). Efforts at Merck on different chemical classes led to the discovery of the brain-penetrant and selective triple blocker MK-8998 (**1**)[25a], which displayed single digit nanomolar activities on the three T-

type calcium channels[25]. This compound was advanced up to a phase II clinical trial for the treatment of acute psychosis in patients with schizophrenia. In this study, **1** was ineffective. However, olanzapine, the active comparator used in this study, displayed only a limited efficacy and therefore the utility of T-channel antagonists to treat schizophrenia cannot be ruled out[26]. Zalicus (now Epirus) discovered Z-944 (**2**)[18], which successfully completed a phase Ib clinical trial. Interestingly, (*R*)-2-(4-cyclopropylphenyl)-*N*-(1-(5-(2,2,2-trifluoroethoxy)pyridin-2-yl)ethyl)acetamide (TTA-A2)[25], a close analog of **1**, and **2** were both assessed and efficacious in rodent models of seizure and epilepsy[18, 27]. Recently, AbbVie reported the discontinuation of their program with the peripherally acting selective triple blocker ABT-639 (**3**)[28] for the treatment of diabetic neuropathies. Additionally, several known antiepileptic drugs, like ethosuximide, phenytoin, valproic acid or zonisamide are claimed to exert at least part of their efficacy through T-type channel inhibition[13, 29].

Figure 1. Triple T-type Calcium Channel Blockers that Have Been Studied in the Clinic

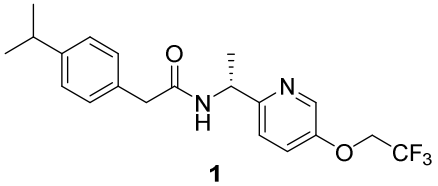

1
MK-8998
(putative structure)
Cav3.1 /3.2 /3.3 IC_{50} [nM] 1.2 / 8.2 / 1.5

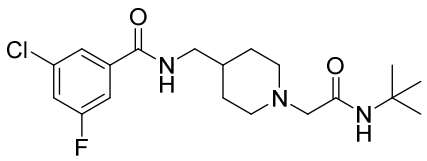

2
Z-944
Cav3.1 /3.2 /3.3 IC_{50} [nM] 37 / 73 / 86

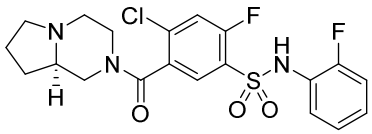

3
ABT-639

Our effort started with an HTS campaign, using a high-throughput calcium flux assay (FLIPR) on cells expressing the recombinant human channels as previously reported[30]. The screening led

to the identification of hit **4** and its close analog **5** (Figure 2). Whereas benzodiazepine **4** exhibited a promising biological activity towards the $Ca_V3.1$, $Ca_V3.2$ and $Ca_V3.3$ channels, a good selectivity over the $Ca_V1.2$ channel, and an acceptable intellectual property position, the compound suffered from a poor solubility, a high lipophilicity, and a low metabolic stability. A metabolite identification was performed to locate soft spots on the molecule. A 10 μM solution of **5** in buffer was incubated for 30 min in the presence of human liver microsomes (HLM) and the formation of two major metabolites was observed (Figure 3). Thus, **5** was debenzylated or oxidized on the benzodiazepine scaffold, leading to the formation of metabolites **6** or **7**, respectively.

Figure 2. Structures of Hits 4 and 5

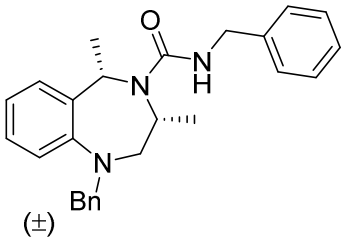

4

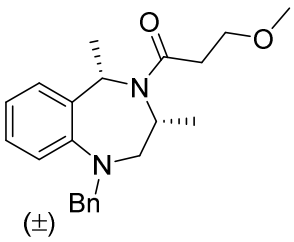

5

	4	**5**
$Ca_V3.1$ /3.2 /3.3 IC_{50} [nM]	17 ± 7 / 35 ± 25 / 8 ± 4	226 ± 82 / 456 ± 165 / 50 ± 10
Solubility [μg/mL] (pH=7/FaSSIF/FeSSIF)	<1 / 6 / 20	27 / 58 / 195
$logD_{7.4}$	>4.1	n.d.
CL_{int} [μL/min/mg] (human/rat)	>1250 / >1250	>1250 / >1250

Figure 3. Structure of Major Metabolites 6 and 7 Observed upon Incubation with HLM

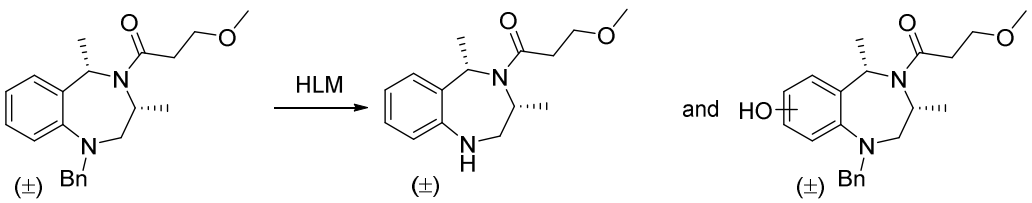

5 **6** **7**

In this work, we present the optimization of racemic hit **4** by reducing its lipophilicity and improving its metabolic stability as well as its solubility resulting in lead compound **(3*R*,5*S*)-31c** which showed promising efficacy in the WAG/Rij-rat model of generalized non-convulsive absence-like epilepsy.

CHEMISTRY

In order to quickly study the structure activity relationship (SAR) around the urea moiety, the replacement of the benzyl group and the substitution of the benzodiazepine scaffold, we developed an efficient synthesis toward the two key building blocks **12** and **13**. As depicted in Scheme 1, our synthesis started with an amide coupling between aminoacetophenone (**8**) and racemic Boc-alanine. A brief survey of activating reagent (EDC•HCl, BTFFH, HATU,…) revealed that the best yields to prepare amide **9** were obtained using $POCl_3$ in pyridine. Substituted aminoacetophenone were also tolerated, allowing the introduction of substituents onto the phenyl of the benzodiazepine core (*vide infra*). The Boc protecting group was cleaved under acidic conditions and the resulting primary amine underwent an intramolecular condensation with the ketone moiety affording imine **10**. The diastereoselectivity of the imine reduction was easily tuned by the choice of the right reaction conditions. Thus, whereas reduction with sodium borohydride led to a 1:1 mixture of the *cis*- and *trans*-isomers, an hydrogenation afforded almost exclusively the *cis*-isomer (***cis*-11**). Notably, the first column chromatography of this synthetic sequence was performed after the imine reduction. Lactam ***cis*-11** was then reduced with borane, and the secondary, aliphatic amine was selectively Boc-protected, leading to the preparation of our first key intermediate **12**. Alkylation with benzyl bromide and subsequent Boc-deprotection yielded the targeted secondary amine **13**.

Scheme 1. Synthesis of the Benzodiazepine Core (Amide Strategy)[a]

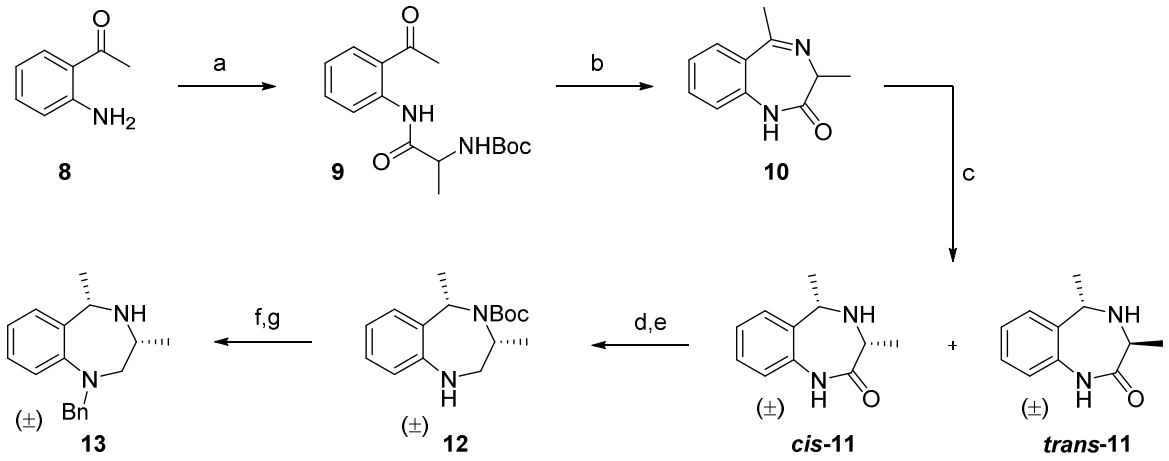

[a] Reagents and conditions: (a) (±)-BocAlaOH, $POCl_3$, pyridine, 0 °C to rt, 2 h, 96%; (b) TFA, DCM, 0 °C to rt, 18 h, 62%; (c) Pd/C, H_2, MeOH, rt, 48 h, 87%; (d) BH_3•DMS, THF, reflux, 18 h, 56%; (e) Boc_2O, Cs_2CO_3, DCM, rt, 3 d, 84%; (f) BnBr, Cs_2CO_3, NaI, DMF, 110 °C, 2 h, 95%; (g) 4M HCl in dioxane, DCM, rt, 6 h, quantitative.

Starting from secondary amine **13**, various urea **14a-d** were synthesized either through reaction with commercially available isocyanates, or from primary amines which were activated with bistrifluoroethoxy carbonate[31]. Amides **15a-d** were conveniently synthesized from the corresponding carboxylic acids using HATU, EDC•HCl, or $POCl_3$ as activating agents (See supporting information for details). Best results were however obtained using HATU as coupling reagent, as exemplified for the synthesis of **15d**. Finally, sulfonamide **16** was obtained through reaction with the corresponding sulfonyl chloride (Scheme 2).

Scheme 2. Urea Variation or Replacement[a]

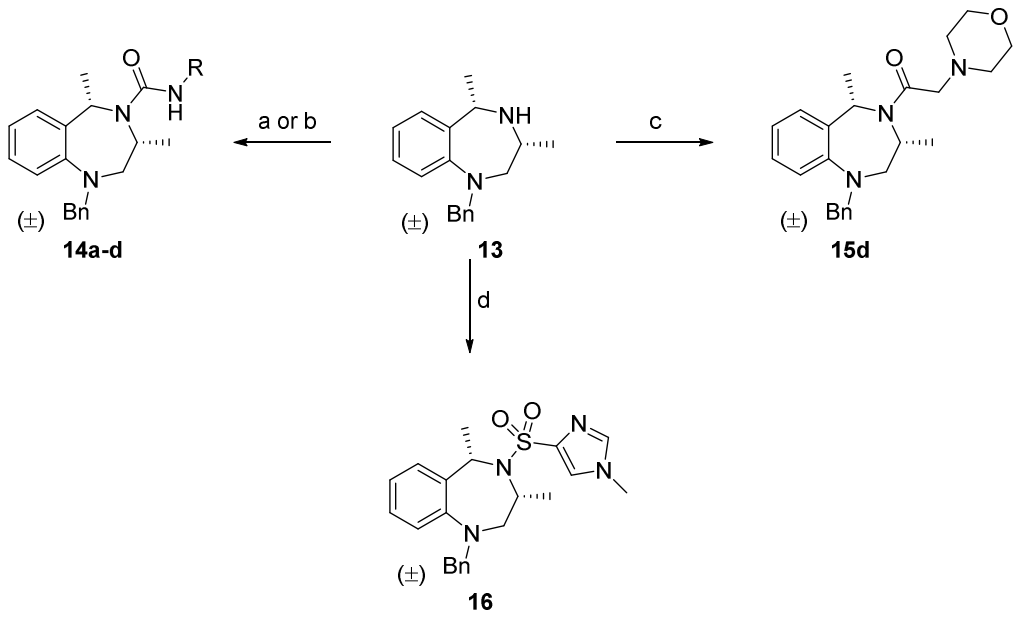

[a] Reagents and conditions: (a) R-NCO, NEt_3, MeCN, rt, 18 h, 24-81%; (b) R-NH_2, $(F_3CCH_2O)_2CO$, DIPEA, MeCN, 75 °C, 2 h, 23%; (c) morpholin-4-yl acetic acid, HATU, NEt_3, DCM, rt, 18 h, 63%; (d) 1-methyl-1*H*-imidazole-4-sulfonyl chloride, NEt_3, DCM, rt, 18 h, 53%.

In order to replace the benzyl moiety, we first alkylated intermediate **12** to obtain compound **17** (Scheme 3). Boc deprotection and subsequent urea formation yielded final compounds **19**. Whereas the alkylation worked nicely under harsh conditions with substituted benzylbromides, erratic yields were obtained with aliphatic- or ether-halides. We eventually discovered that variation could easily by introduced through reductive amination between intermediates **12** or **18**[32] and an aldehyde. As all desired aldehydes could not be synthesized, we turned our attention to the methodology reported by Sorribes *et al*.[33]. Thus, in the presence of the Karstedt's catalyst, carboxylic acids were suitable substrates to alkylate intermediates **12**. Alternatively, intermediate **12** was subjected to Buchwald-Hartwig cross coupling, acylation, or treated with a sulfonyl

chloride to give, after Boc deprotection and urea formation, final products **19v**, **19w**, or **19x** respectively (see Table 3).

Scheme 3. Benzyl Variation[a]

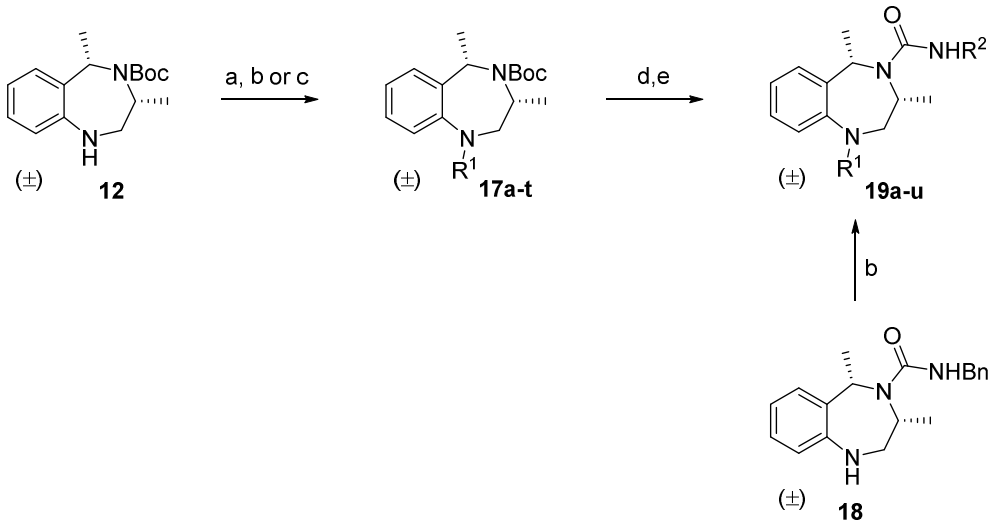

[a] Reagents and conditions: (a) R^1-Br, DIPEA, DMF, 180 °C (μW), 15 min, 26-90%; (b) R^1-CHO, $NaBH(OAc)_3$, DCE, 50 °C, 2 h, 6-95%; (c) R^1-CO_2H, $PhSiH_3$, dppe, [Pt] Karstedt's catalyst, $n$$Bu_2O$, 60 °C, 18 h, 59%; (d) TFA, DCM, 0 °C to rt, 18 h, 97%-quantitative; (e) BnNCO or pyridine-3-isocyanate, NEt_3, DCM or MeCN, 0 °C, 1 h, 13-95%.

Synthesis of phenyl substituted benzodiazepines **20-25** (Table 4) were performed either from the corresponding substituted aminoacetophenone as previously mentioned and described in Scheme 1 and 2, or by late state functionalization of bromide **21**[32]. Thus, cyanation of the aryl halide following Rosenmund- von Braun[34-38] protocol led to nitrile derivative **22**, while treatment with trifluoroethanol and NaH in presence of $CuBr_2$[39] gave the corresponding ether **23** (Scheme 4). Alternatively, a Negishi coupling allowed for introduction of a methyl group **(24)** whereas a L-proline-promoted CuI-catalyzed coupling between **21** and sodium methanesulfinate [40, 41] gave aryl sulfone **25**.

Scheme 4. Phenyl Ring Substitution[a]

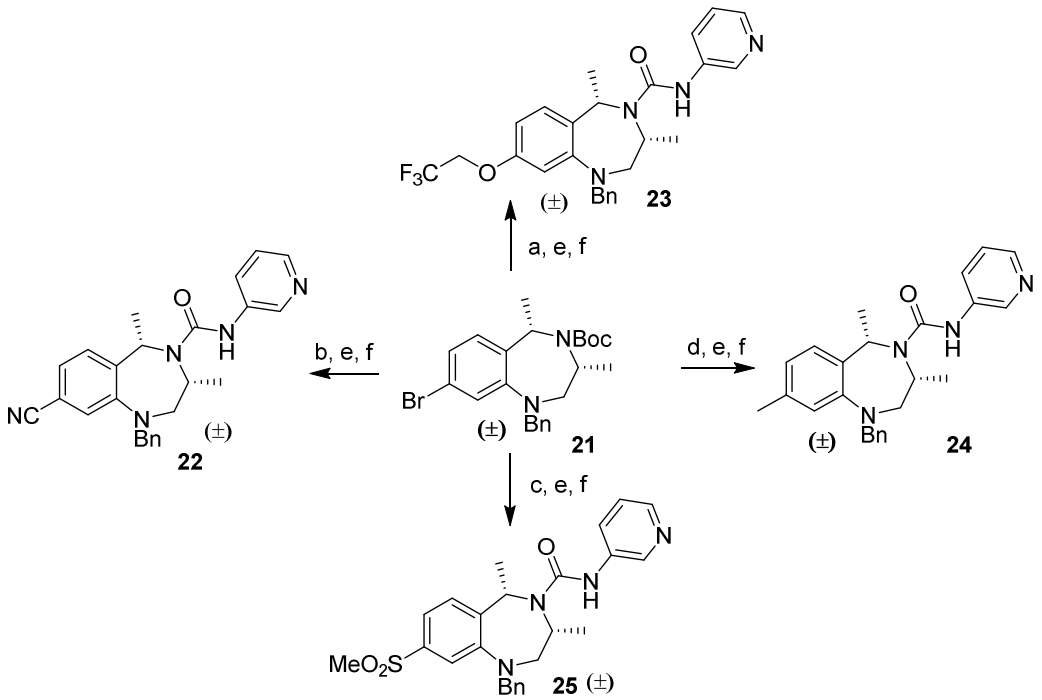

[a] Reagents and conditions: (a) $CuBr_2$, NaH, CF_3CH_2OH, DMF, 110 °C, 18 h, 58%; (b) ZnCN, Pd_2dba_3, dppf, PMHS, DMAC, 150 °C (μW), 40 min, 36%; (c) $NaSO_2Me$, L-Proline, CuI, DMSO, 110 °C, 48 h, 47%; (d) Me_2Zn, $Pd(PPh_3)_4$, THF, 50 °C, overnight, 68%; (e) 4M HCl dioxane, rt, overnight, **22** (quantitative), **23** (quantitative), **24** (quantitative), **25** (quantitative); (f) pyridine-3-isocyanate, NEt_3, MeCN, overnight, **22** (71%), **23** (64%), **24** (84%), **25** (85%).

Apart from the classical amide coupling-cyclization-reduction strategy, a second approach for the construction of the pyridodiazepinic core structure is represented in Scheme 5a and involves an aromatic nuclophilic substitution (S_NAr) as a key step. The synthesis of derivative **31c** is reported as example. Reaction between 3-fluoroisonicotinonitrile (**26**) and primary amine **27**[42] led to pyridine **28**, which was in turn converted into the corresponding methyl ketone upon treatment with MeLi in THF. Boc deprotection led to imine **29**, which was susbequently benzylated on the anilic nitrogen using NaH as a base and benzyl bromide in DMF at 70 °C.

Hydrogenation of the imine with Pd/C yielded **30** with a *cis/trans* diastereoselectivity of 9:1. The two diastereoisomers could be easily separated by column chromatography and ***cis*-30** was submitted to urea formation under standard conditions to afford **31c**. Alternatively, the alkyl side chain could be introduced from the beginning of the sequence. For example secondary amine **33**[43] was reacted with 3,5-difluoroisonicotinonitrile (**32**) to give **34** (Scheme 5b). The synthesis continued as described for **31c** to afford **31l** in a 5 steps sequence. Interestingly, hydrogenation of the imine with Pd/C was found to be ineffective when F was present, while changing the catalyst to PtO_2 led to the formation of the *anti*-stereoisomer as the major product (*cis*/*trans* 4:6). Finally, reduction with sodium triacetoxyborohydride resulted in a 1:1 *cis*/*trans* ratio. These two approaches were not limited to the synthesis of pyridyldiazepines only but could also be applied for the synthesis of some phenyl substituted benzodiazepines.

Scheme 5. Synthesis of the Benzodiazepine Pyridine Core (S_NAr Strategy)[a]

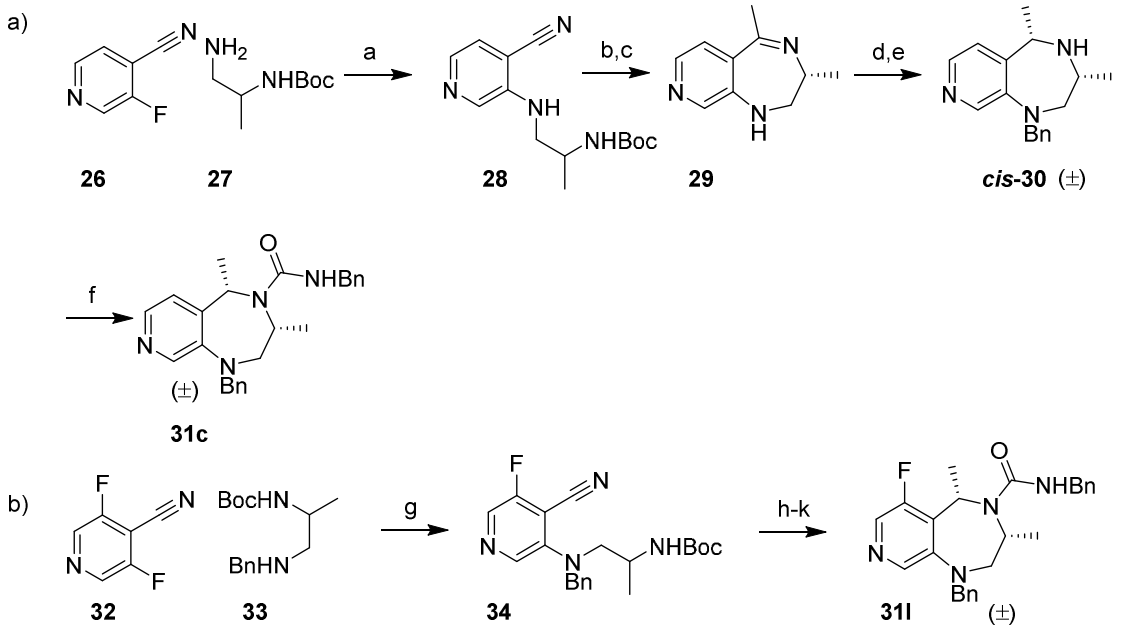

[a] Reagents and conditions: (a) NEt_3, NMP, 90 °C, overnight, 85%; (b) MeLi, THF, 0 °C to rt, overnight, 52%; (c) 4M HCl in dioxane, rt, overnight, 100%; (d) NaH, BnBr, DMF, 70 °C, 2 h, 60%; (e) Pd/C, H_2, MeOH, rt, 90 min, 77%; (f) BnNCO, DIPEA DCM, rt, overnight, 80%; (g) NMP, DIPEA 120 °C, overnight, 69%; (h) MeLi, THF, -78 °C to 0 °, overnight, 25%; (i) 4M HCl in dioxane, rt, 1 h, 98%; (k) $NaBH(OAc)_3$, MeOH, rt, 1 h, 27% *cis*-isomer, 27% *trans*-isomer; (l) BnNCO, DIPEA DCM, rt, overnight, 34%.

RESULTS AND DISCUSSION

The optimization work started by assessing the importance of the two *cis*-methyl groups on the benzodiazepine core. To this end, a methyl scan was performed (Table 1). Removal of one or of both methyl groups led to a significant loss in potency, as could be observed for compounds **35a**, **35b**, or **35c**. Displacing a methyl from the 3- to the 2-position of the benzodiazepine scaffold was also detrimental and both *cis*- or *trans*-analogs **35d** or **35e** were not further pursued. The corresponding *trans*-isomer of initial hit (**4**), **35f**, was also clearly less active. Finally, switching to a benzodiazepinone scaffold, as exemplified with **35g** or **36**, was not well tolerated either. In conclusion, the two methyl groups in a *cis*-conformation were required to achieve a suitable biological potency. Importantly, derivatives **35a-g** and **36** were all found to be metabolically unstable.

Next, optically pure enantiomers **(3*S*,5*R*)-4** and **(3*R*,5*S*)-4** were synthesized. A chiral resolution of racemic intermediate ***cis*-17** using a column charged with a chiral stationary phase afforded enantiomers **(3*S*,5*R*)-17** and **(3*R*,5*S*)-17** (Scheme 6). The Boc protecting group was cleaved under acidic conditions to give optically pure secondary amines **(3*S*,5*R*)-13** and **(3*R*,5*S*)-13**

which were converted into final compounds **(3*S*,5*R*)-4** or **(3*R*,5*S*)-4** upon treatment with benzyl isocyanate. Enantiomer **(3*R*,5*S*)-4** was found more potent than the other one. To determine the absolute configuration of the most potent enantiomer, amine **(3*S*,5*R*)-13** (precursor of the less active enantiomer) was converted into biologically inactive Mosher's amide **(3*S*,5*R*)-37** upon treatment with (*S*)-(+)-α-methoxy-α-trifuloromethylphenylacetyl chloride. By slow diffusion of pentane into a concentrated solution of **(3*S*,5*R*)-37** in diethyl ether, suitable single crystals were obtained to carry out an X-ray crystal structure analysis, leading to the conclusion that the most active enantiomer presented the (3*R*,5*S*) dimethyl conformation. For the sake of convenience, most of the optimization work was however performed using racemic material (see below).

Table 1. Core Modification: Importance of the two Methyl Groups

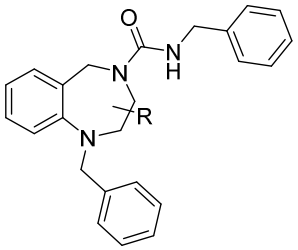

35a-g

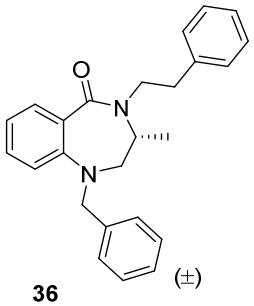

36

Cmpd.	R	Ca_v 3.1 Ca_v 3.2 Ca_v 3.3 IC_{50} (nM) [a]	Cl_{int} HLM (µL/min/mg)[b]	Cmpd.	R	Ca_v 3.1 Ca_v 3.2 Ca_v 3.3 IC_{50} (nM)[a]	Cl_{int} HLM (µL/min/mg)[b]
4 (Ref.)	---	17 ± 7 35 ± 25 8 ± 4	>1250	**35f**	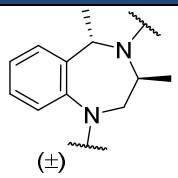 (±)	279 ± 55 340 ± 340 95 ± 34	>1250

35a	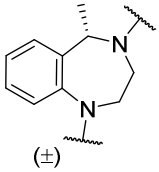 (±)	193 ± 26 241 ± 98 164 ± 51	>1250	**35g**	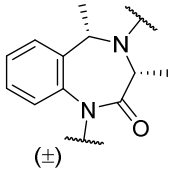 (±)	304 ± 109 682 ± 266 259 ± 132	>1250
35b	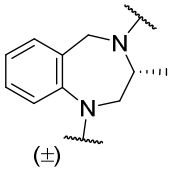 (±)	102 ± 19 141 ± 25 26 ± 9	>1250	**36**	---	676 ± 292 618 ± 334 1589 ± 696	>1250
35c	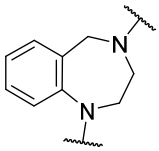	305 ± 58 392 ± 158 214 ± 77	>1250	**(3*S*,5*R*)-4**	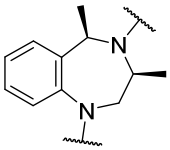	262 ± 74 358 ± 138 641 ± 101	n.d.
35d	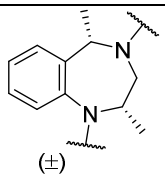 (±)	293 ± 27 464 ± 248 1003 ± 144	n.d.	**(3*R*,5*S*)-4**	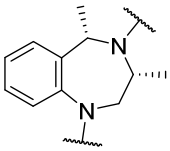	5 ± 1 17 ± 10 2 ± 0.1	n.d.
35e	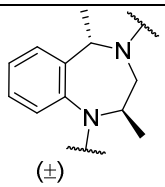 (±)	211± 31 198 ± 88 326 ± 279	n.d.				

[a] Values represent the average of at least three independent runs. [b] n= 1.

Scheme 6. Synthesis of Mosher's Amide (3*S*,5*R*)-37[a]

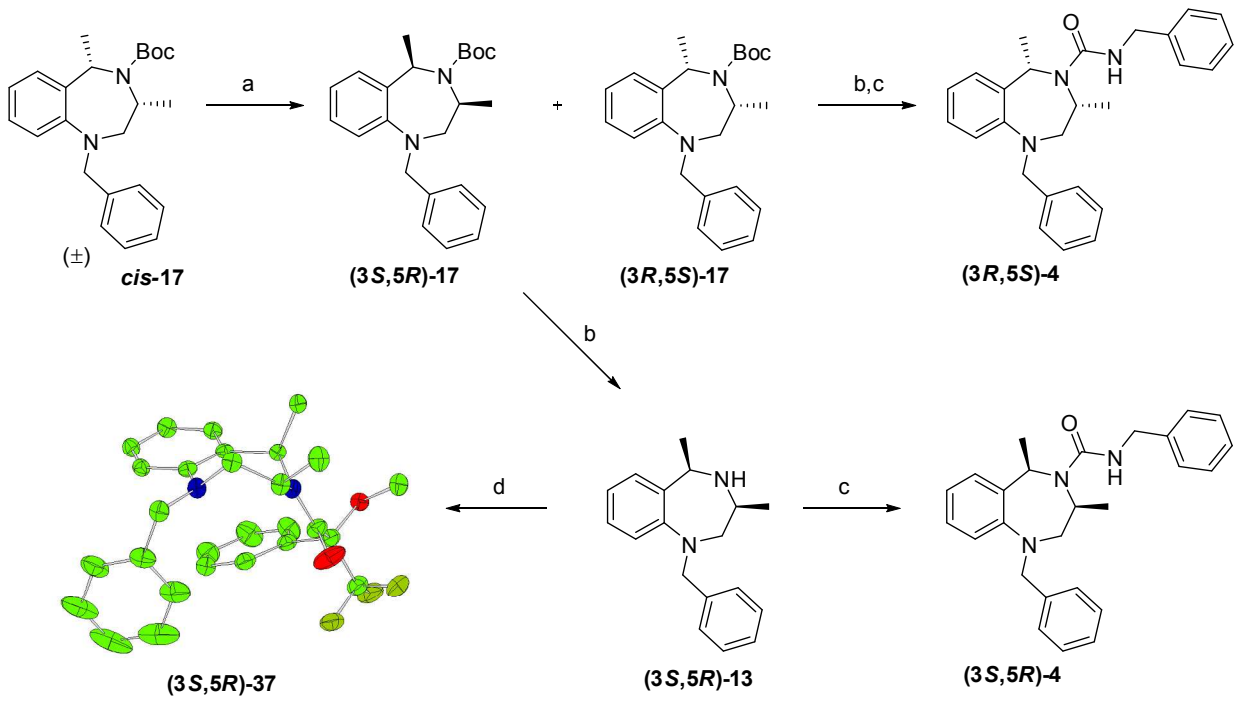

[a] Reagents and conditions: (a) Prep. chiral HPLC (column (*R*,*R*) Whelk-O1, heptane:EtOH/0.1%DEA 1:9), **(3*S*,5*R*)-17** (46%), **(3*R*,5*S*)-17** (48%); (b) 4M HCl in dioxane, EtOH, rt, 2 d, quantitative; (c) BnNCO, NEt_3, MeCN, rt, 18 h, 65-76%; (d) (*S*)-(+)-α-methoxy-α-trifuloromethylphenylacetyl chloride, DIPEA, DCM, rt, 2 d, 45%.

Next, modification of the benzyl urea moiety (Table 2) demonstrated that this region of the molecule is fairly tolerant. Indeed, several ureas **14a-d** or amides **15a-d** led to potent compounds. Notably, polar groups like an oxetane or pyridine were suitable substrates and helped to tune the physicochemical properties of the final compounds (*vide infra*). Alkylation of the urea moiety resulted in loss of activity, as can be seen for compound **38**. Sulfonamides or carbamates were clearly less potent, as exemplified with **16** or **39**. Finally, a carbonyl function was absolutely mandatory to retain a good biological activity, as tertiary basic amine like derivative **40** were inactive.

Whereas several amides or ureas proved to be well tolerated and afforded potent triple blockage, these replacements did not lead to significant improvement in the intrinsic clearance. However, solubility of the compounds was markedly enhanced by the introduction of an heterocycle or an ether moiety and compounds **14b**, **14c**, or **15c** exhibited a solubility ranging from 21 to 39 µg/mL at pH 7. The most interesting compound identified during the replacement of the benzyl urea was oxetane analog **14d**, for which both solubility (148 µg/mL at pH 7) and human metabolic stability (539 µL/min/mg) were significantly improved.

Table 2: Variation of the Urea Moiety

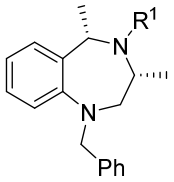

(±)

Cmpd.	R^1	Ca_v 3.1 Ca_v 3.2 Ca_v 3.3 IC_{50} (nM)[a]	Cl_{int} HLM (µL/min/mg)[b]	Cmpd.	R^1	Ca_v 3.1 Ca_v 3.2 Ca_v 3.3 IC_{50} (nM)[a]	Cl_{int} HLM (µL/min/mg)[b]
4 (Ref.)	-	17 ± 7 35 ± 25 8 ± 4	>1250	**15c**	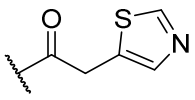	34 ± 4 55 ± 25 6 ± 1.6	>1250
14a	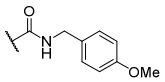	8 ± 2 14 ± 1.5 6 ± 2	>1250	**15d**	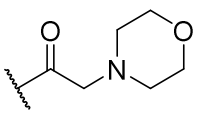	36 ± 18 51 ± 15 7 ± 5	>1250

14b	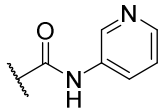	42 ± 24 61 ± 24 14 ± 3	>1250	**16**	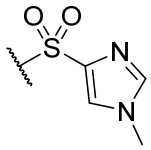	576 ± 6 1490 ± 11 210 ± 9	n.d.
14c	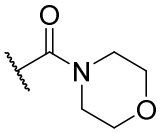	26 ± 4 58 ± 13 9 ± 3	>1250	**38**	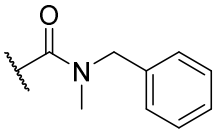	457 ± 212 835 ± 403 892 ± 255	n.d.
14d	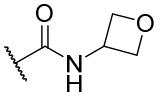	26 ± 9 61 ± 20 12 ± 2	539	**39**	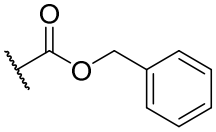	420 ± 114 841 ± 200 325 473± 27	n.d.
15a	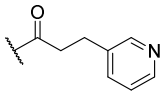	31 ± 4 38 ± 18 10 ± 3	>1250	**40**	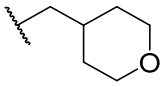	6110 ± 13.4 7410 ± 47 >10000 ± 9	n.d
15b	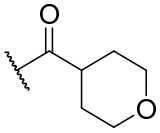	24 ± 9 47 ± 31 8 ± 4	1160				

[a] Values represent the average of at least three independent runs. [b] n=1.

As mentioned earlier, debenzylation was identified as the main mechanism of metabolism. Several replacements were therefore introduced to block this soft spot. Substitution of the benzyl moiety with one (compounds **19a**, **19b**, or **19c**) or two fluorine atoms (compounds **19d** or **19e**) led to very potent triple T-type calcium channel blockers. Replacement of the phenyl moiety with unsubstituted pyridines resulted in less active analogs (e.g. **19f**, **19g**, or **19h**). In the case of 2- or 3-pyridines, the activity was recovered by the introduction of a suitable substituent (see **19i**, **19j**, or **19k**). The most potent triple T-type calcium channel blockers of this work were identified by the introduction of substituted 5-membered heterocycles, like furane derivatives **19l** or **19m**, or thiazoles **19n** or to a lesser extent **19o**. Bulky alkyl chains or even cycloalkyl groups could

also be tolerated whereas less hindered alkyl chains showed lower potencies. Thus, whereas ethyl derivative **19p** was not very potent, isopentyl **19q** or cyclopentyl **19r** displayed an interesting biological activity. Finally, we introduced ether moieties, as exemplified by derivatives **19s**, **19t**, or **19u**. Notably, the introduction of this more polar moieties resulted in a remarkable improvement in solubility (248 μg/mL at pH 7 for **19s** or 81 μg/mL at pH 7 for **19t**).

Whereas several suitable replacements for the benzyl groups led to potent compounds and enhanced in some cases the solubility, none of these were able to prevent metabolic degradation. We therefore removed the -CH_2- linker, but the resulting phenyl analog **19v** was metabolically unstable. Introduction of an amide (**19w**) or a sulfonamide (**19x**) resulted in a massive loss in potency. Attempts to hinder the metabolism by deuterium introduction[44] (**19y**) were also unsuccessful. Finally, only the inactive debenzylated analog **18** proved to be metabolically stable when incubated with HLM.

Table 3. Replacement of the Benzyl Moiety

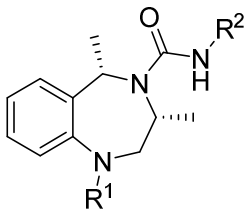

(±)

Cmpd.	R^1	R^2	Ca_v 3.1 Ca_v 3.2 Ca_v 3.3 IC_{50} (nM)[a]	Cl_{int} HLM (μL/min /mg)[c]	Cmpd.	R^1	R^2	Ca_v 3.1 Ca_v 3.2 Ca_v 3.3 IC_{50} (nM)[a]	Cl_{int} HLM (μL/min /mg)[c]

4 **(Ref.)**	---	---	17 ± 7 35 ± 25 8 ± 4	>1250	**19n**	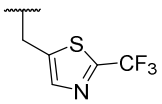	Bn	13 ± 6 15 ± 6 6 ± 2	>1250
19a	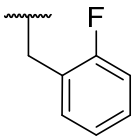	3-Py	4 ± 1 11 ± 2.5 5 ± 3	1200	**19o**	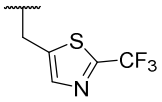	3-Py	33 ± 7 42 ± 9 33 ± 18	>1250
19b	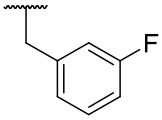	3-Py	8 ± 2 14 ± 3 5 ± 2	>1250	**19p**		Bn	754 ± 225 922 ± 346 139 ± 56	>1250
19c	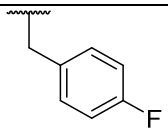	3-Py	25 ± 6 31 ± 7 7 ± 2	>1250	**19q**	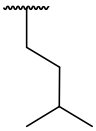	3-Py	23 ± 14 91 ± 53 12 ± 7	>1250
19d	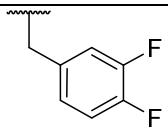	3-Py	13 ± 2 18 ± 14 6 ± 2	>1250	**19r**	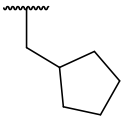	3-Py	23 ± 5 62 ± 13 14 ± 4	1150
19e	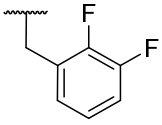	Bn	5 ± 1 9 ± 1 4 ± 0.3	n.d.	**19s**	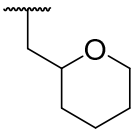	3-Py	875 ± 325 [b] 2670 ± 980 [b] 243 ± 77 [b]	720
19f	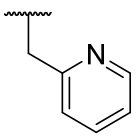	Bn	605 ± 216 479 ±	n.d.	**19t**	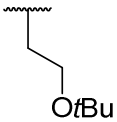	3-Py	108 ± 12 91 ± 20 23 ± 8	1230

			274 97 ± 26						
19g	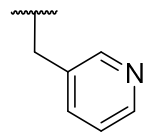	Bn	476 ± 246 500 ± 206 95 ± 6	n.d.	**19u**	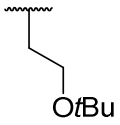	Bn	35 ± 17 44 ± 12 12 ± 3	n.d.
19h	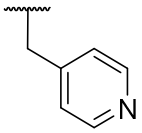	Bn	>7260[b] ± 3874 >8580[b] ± 3705 1710[b] ± 650	n.d.	**19v**	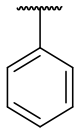	Bn	256 ± 20 209 ± 55 225 ± 73	>1250
19i	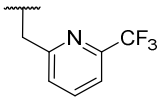	Bn	25 ± 5 42 ± 8 14 ± 6	>1250	**19w**	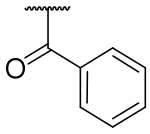	Bn	6070 ± 400[b] >11550 ± 1250[b] >10000[b]	n.d.
19j	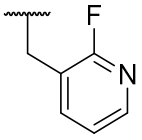	Bn	53 ± 20 49 ± 1 10 ± 2	>1250	**19x**	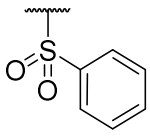	3-Py	>10000[b] 4695[b] ± 1985 1810[b] ± 350	n.d.
19k	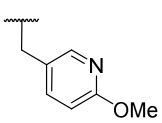	Bn	45 ± 5 33 ± 5 10 ± 3	>1250	**19y**	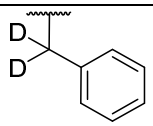	3-Py	27 25 4	1110

19l	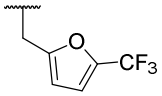	Bn	7 ± 1.4 13 ± 2 6 ± 1	>1250	**18**		Bn	>10000[b] >10700[b] >8605[b]	59
19m	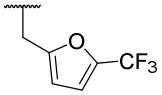	3-Py	4 ± 1 14 ± 5 9 ± 6	>1250					

[a] Values represent the average of at least three independent runs unless otherwise stated. [b] n=2. [c] n=1.

After modification of the urea and replacement of the benzyl moiety we concentrated our efforts on the benzodiazepinic scaffold with the following goals: keep a high potency on the $Ca_V3.1$, $Ca_V3.2$, and $Ca_V3.3$ T-type channels, decrease the lipophilicity of the molecule and block the metabolically weak spots. First, we studied the effect of the substitution of the phenyl ring on activity and on human liver microsomal stability (Table 4). In this regard fluorine resulted to be the best substituent. In particular, incorporation of a fluorine atom at position R^1 (**20a**) allowed to keep comparable activity to reference compound **4** while moderately improving HLM intrinsic clearance. On the other hand, fluorine substitution at R^2 (**20b**), or R^3 (**20c**) gave potent compounds that remained unstable in HLM. Finally, introduction of a fluorine at position R^4 (**20d**) allowed to improve the HLM intrinsic clearance but resulted in a considerable decrease in the IC_{50} values. The substitution with more polar or bulkier groups such as -OMe, -CN, $-SO_2Me$, $-OCH_2CF_3$ led to an important loss in potency even though in some cases improved HLM values were observed (**20g**, **20h** and **22**). In general, the substitution of the benzodiazepinic phenyl ring showed to be sensitive and provided no substantial improvement of metabolic stability in human liver microsomes without substantially reducing activity. Furthermore, in none of the examples the rat liver microsomal intrinsic clearance (RLM) could be improved (RLM >1250 μL/min/mg).

Table 4: Activities and Microsomal Stability of Phenyl Substituted Benzodiazepines

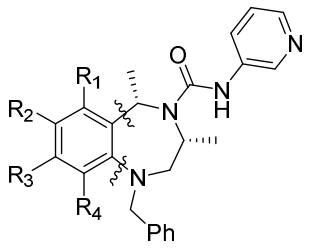

(±)

Cmpd.	Scaffold	Ca_v 3.1 Ca_v 3.2 Ca_v 3.3 IC_{50} (nM)[a]	Cl_{int} HLM (µL/min/mg)[c]	Cmpd.	Scaffold	Ca_v 3.1 Ca_v 3.2 Ca_v 3.3 IC_{50} (nM)[a]	Cl_{int} HLM (µL/min/mg)[c]
4 (Ref.)	---	17 ± 7 35 ± 25 8 ± 4	>1250	**20h**	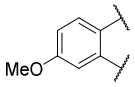	627 ± 460 1600 ± 961 610 ± 201	649
20a		20 ± 9 52 ± 18 10 ± 3	628	**20i**	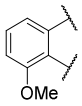	>5300 >6500 >9000	n.d.
20b	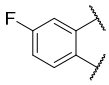	68 ± 29 112 ± 35 8 ± 3	>1250	**20j**	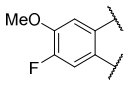	370 ± 46 414 ± 111 73 ± 27	n.d.
20c	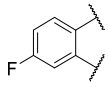	6 ± 1 12 ± 4	>1250	**20k**	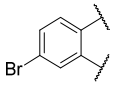	286 ± 21 428 ± 43	n.d.

		4 ± 1				137 ± 81	
20d	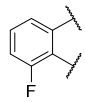	178 ± 37 205 ± 137 17 ± 5	720	**22**	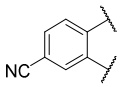	582 ± 4[b] 860 ± 391[b] 308 ± 84 [b]	418
20e	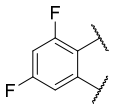	12 ± 2 22 ± 14 8 ± 5	873	**23**	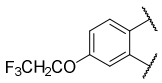	187 ± 104 790 ± 289 3557 ± 1690	>1250
20f	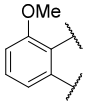	188 ± 94 305 ± 93 130 ± 69	n.d.	**24**	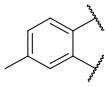	227 ± 21 231 ± 64 74 ± 54	n.d.
20g	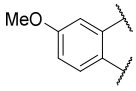	390 ± 80 530 ± 125 100 ± 29	521	**25**	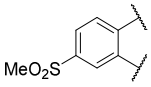	>10000 >8000 >10000	n.d

[a] Values represent the average of at least three independent runs unless otherwise stated. [b] n= 2. [c] n= 1.

Driven by the observation that a fluorine atom on the phenyl ring could moderately stabilize the molecule, we further investigated this effect on the so far best combinations (Table 5). If on one hand the substitution with a fluorine led to an important lowering of the HLM values for **41**, on

the other hand it was able to only moderately stabilize compounds showing already interesting *in vitro* clearance (**43** vs. **42**, **45** vs. **44** and **46** vs. **14d**).

Table 5: Effect of Fluorine Substitution on HLM

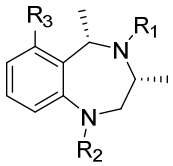

(±)

Cmpd.	R1	R2	R3	Ca_v 3.1 Ca_v 3.2 Ca_v 3.3 IC_{50} (nM)[a]	Cl_{int} HLM (µL/min/ mg)[b]
4 (Ref.)	---	---	---	17 ± 7 35 ± 25 8 ± 4	>1250
15a	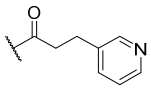	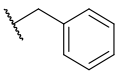	H	31 ± 4 38 ± 18 10 ± 3	>1250
41	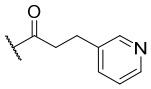	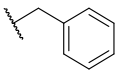	F	47 ± 15 52 ± 11 17 ± 5	562
42	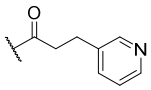	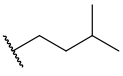	H	29 ± 14 62 ± 22 13 ± 3	412

43	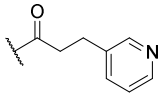	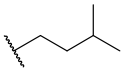	F	45 ± 21 66 ± 18 52 ± 13	357
44	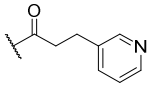	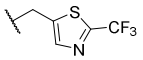	H	40 ± 12 30 ± 10 13 ± 5	332
45	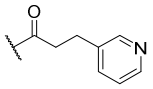	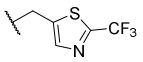	F	115 ± 53 93 ± 40 20 ± 8	193
14d	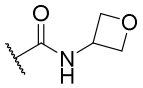	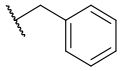	H	26 ± 9 61 ± 20 12 ± 2	539
46	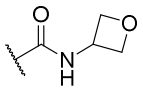	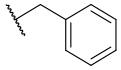	F	40 ± 15 59 ± 14 13 ± 6	375

[a] Values represent the average of at least three independent runs. [b] n= 1.

With the goal to further stabilize our derivatives against phase I metabolism, we modified the benzodiazepinic scaffold replacing the phenyl ring portion by six- and five membered ring heterocycles (Table 6). Pyridodiazepine derivatives **31a** and **31b** proved to be only moderately active or inactive compared to **4** respectively, while **31c** and **31d** showed interesting activity on the three channels. Importantly, **31c** presented an encouraging *in vitro* clearance of 276 µL/min/mg. We therefore studied the effect of the substitution of these two pyridodiazepine derivatives on HLM stability and on activity on the T-type calcium channels. For the pyridodiazepines with *N* at 9-position (**31d**), the substitution in *ortho* with –Cl (**31e**), –F (**31g**),

and –Me (**31i)** did improve neither the already excellent activity nor the metabolic stability, whereas the substitution with a $–CF_3$ led to a moderate improvement in HLM stability but also to a loss in potency (**31j**). The introduction of substituents at 7-position (**31f** and **31h**) could moderately stabilize the molecule while keeping acceptable IC_{50} values. Nevertheless, the most interesting results were obtained with pyridodiazepines with *N* at 8-position. In particular **31l** where a fluorine atom was introduced in *meta* position displayed the lowest HLM stability while keeping an acceptable potency on the $Ca_v3.1$, -3.2 and -3.3 T-type channels. Lastly, pyrimidodiazepine **31n** and pyrazolodiazepine **31o** were inactive on the target. However, in none of the examples the RLM stability could be improved by introducing an heterocycle (RLM >1250 μL/min/mg).

With **31c** and **31l** in our hands, we investigated the replacement of the benzyl moiety and the modification of the urea part (Table 7). In contrast to the 1,4-benzodiazepines with the naked scaffold, 1,4-pyridodiazepines were less active upon ureas replacement with amides and at the same time the HLM stability dropped considerably (e.g. **47**). Compared to parent benzodiazepine **31c**, bis deuterated benzodiazepine **48** showed a slightly improved metabolic stability in presence of HLM. Introduction of a trifluoromethylfurane moiety instead of a benzyl group allowed to improve the potency (**52**) while keeping the HLM stability constant, whereas the introduction of *o*,*m*-difluorobenzyl- or *o*-fluorobenzyl-substituents allowed at the same time to boost the activity and to improve further the HLM stability (**49** and **50**).

Table 6: Benzodiazepinic Core Modification by Incorporation of Heterocycles

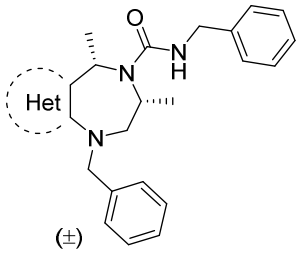

Cmpd.	Scaffold	Ca_v 3.1 Ca_v 3.2 Ca_v 3.3 IC_{50} (nM)[a]	Cl_{int} HLM (µL/min/mg)[c]	Cmpd.	Scaffold	Ca_v 3.1 Ca_v 3.2 Ca_v 3.3 IC_{50} (nM)[a]	Cl_{int} HLM (µL/min/mg)[c]
4 (Ref.)	---	17 ± 7 35 ± 25 8 ± 4	>1250	**31h**	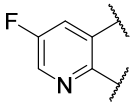	65 ± 12 95 ± 9 15 ± 6	837
31a	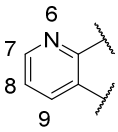	597 ± 29 212 ± 23 91 ± 24	n.d	**31i**	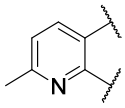	18 ± 5 28 ± 4 33 ± 9	1240
31b	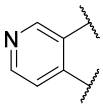	6280 ± 1670[b] >11000[b] >8740[b]	n.d.	**31j**	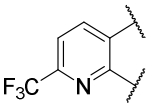	57 ± 15 104 ± 11 281 ± 78	531
31c	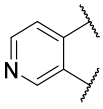	142 ± 52 236 ± 89 25 ± 10	276	**31k**	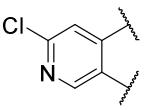	220 ± 20 224 ± 52 55 ± 19	>1250

31d	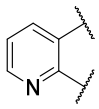	15 ± 3 31 ± 16 8 ± 3	1060	**31l**	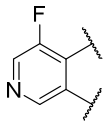	140 ± 9 72 ± 11 9 ± 7	185
31e	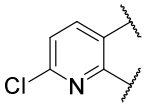	16 ± 5 36 ± 7 22 ± 12	1005	**31m**	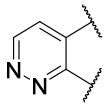	1139 ± 333 695 ± 346 206 ± 29	n.d.
31f	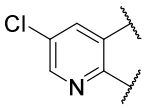	78 ± 10 68 ± 25 46 ± 18	409	**31n**	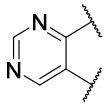	>8500 >6400 1000 ± 316	n.d
31g	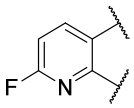	7 ± 1 6 ± 1 4 ± 0.2	>1250	**31o**	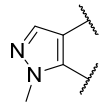	>9400[b] >7300[b] >10000[b]	n.d.

[a] Values represent the average of at least three independent runs unless otherwise stated. [b] n=2 . [c] n= 1.

Interestingly, the *p*-methoxybenzyl urea improved both the activity and the intrinsic clearance in human liver microsomes at once as shown in **51**. Keeping the urea part fixed and replacing the aromatic benzyl group by an isopentyl allowed to significantly improve the metabolic stability in HLM without observing a drop in the activity (**54**). The combination of the *p*-methoxybenzyl urea with the trifluoromethylfurane led to benzodiazepine **53** which presented an excellent activity on all three T-type calcium channels, similar stability in presence of HLM but also improved stability in RLM compared to **51**. Similarly, in derivative **55** the introduction of the 3-

pyridyl urea allowed to ameliorate the HLM stability by a factor 3 and also to improve considerably the RLM stability. Hindering the metabolism by the introduction of deuterium at the benzylic position, allowed to improve slightly the metabolic stability in HLM (**56**). Once again the replacement of the benzyl substituent by an isopentyl group (**58**) allowed to stabilize the molecule in human liver microsomes by a factor 2 and the introduction of a fluorine substituent *meta* to the *N* atom allowed to improve the IC_{50}, especially of the Ca_v 3.2 T-channel type (**57**). Nonetheless, beside the clear drop in activity, an important drawback of 3-pyridyl ureas **55**, **57** and **58** was the low brain penetration potential across the blood brain barrier (BBB). Indeed, we measured a set of pyridodiazepines in the MDR1/MDCK assay which allows evaluation of passive permeability and potential interaction with human drug efflux P-glycoprotein transporter (Figure 4). Derivative **31c** showed an acceptable value for the efflux ratio (P_{app} basolateral to apical (BA)/ P_{app} apical to basolateral (AB)) of 3.2 and a good passive permeability (P_{app} (AB) = 16.6 (10^{-6} cm/s)) indicating that the compound is a weak substrate for human P-gp and has the potential to cross the BBB. In **31l**, the introduction of a fluorine atom allowed to lower the pyridine's basic pKa by two logunits (from 6.2 to 4.2) resulting in an improved efflux ratio of 2.3 with good passive permeability P_{app} (AB) = 26.3 (10^{-6} cm/s). Nonetheless, replacement of the benzyl urea by the 3-pyridyl urea resulted in a benzodiazepine (**57**) showing a high efflux ratio of 60 suggesting that this compound is a strong substrate of human P-gp. The similarity in the logD values between **31c** and **57** (3.1 and 3.3 respectively) suggests that the introduction of a second basic center with a pKa≅ 4.4 is detrimental for the permeation.

Table 7: Best Pyridodiazepine Derivatives

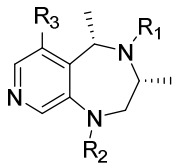

(±)

Cmpd.	R1	R2	R3	Ca_v 3.1 Ca_v 3.2 Ca_v 3.3 IC_{50} (nM)[a]	Cl_{int} HLM (µL/min/mg)[b]	Cl_{int} RLM (µL/min/mg)[b]
4 (Ref.)	---	---	---	17 ± 7 35 ± 25 8 ± 4	>1250	>1250
47	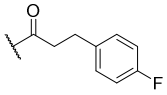	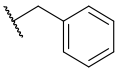	H	196 ± 80 225 ± 29 25 ± 5	907	>1250
48	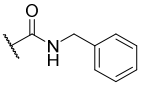	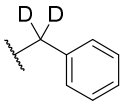	H	260 ± 46 230 ± 21 15 ± 3	186	>1250
49	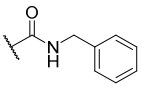	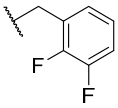	H	38 ± 11 72 ± 25 13 ± 1	212	n.d.
50	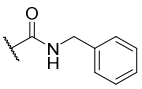	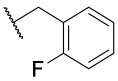	H	47 ± 14 95 ± 18 31 ± 21	179	>1250
51	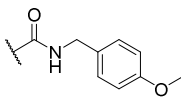	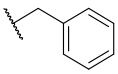	H	79 ± 21 48 ± 11 12 ± 4	189	1140

52	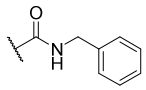	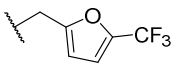	H	37 ± 9 44 ± 23 10 ± 3	247	1180
53	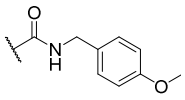	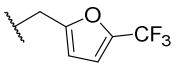	H	13 ± 1 24 ± 3 11 ± 2	119	447
54	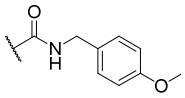	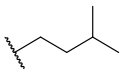	H	76 ± 4 55 ± 14 25 ± 6	94	885
55	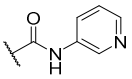	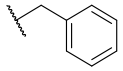	H	360 ± 237 860 ± 158 306 ± 72	93	562
56	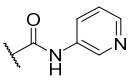	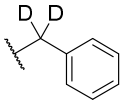	H	441 ± 115 815 ± 135 148 ± 15	59	855
57	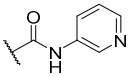	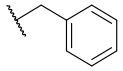	F	107 ± 30 240 ± 65 133 ± 34	83	500
58	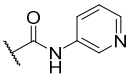	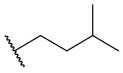	H	613 ± 63 604 ± 52 251 ± 48	30	496

[a] Values represent the average of at least three independent runs. [b] n= 1.

Figure 4. LogD, MDR1/MDCK1, Solubility and pKa of Pyridodiazepines

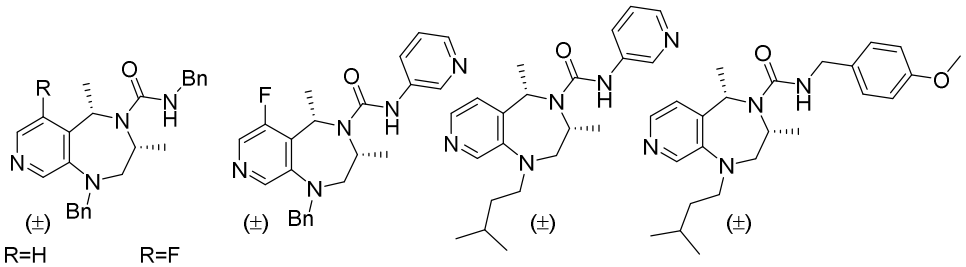

	31c	**31l**	**57**	**58**	**54**
$LogD_{7.4}$	3.1	n.d	3.3	3.2	4.0
Papp AB (10^{-6} cm/s)	16.6	26.3	0.9	0.4	10.6
Papp BA (10^{-6} cm/s)	55.8	61.0	53.8	56	54.5
BA/AB ratio	3.4	2.3	60	140	5.1
Solubility pH7 [μg/mL]	42	n.d	177	309	9
pKa	6.2	4.2	3.8/4.7	4.4/6.3	6.4

In Vivo Pharmacology with Compound 31c

After having improved the physicochemical and *in vitro* DMPK properties of the series, we assessed the efficacy of this chemical class in the WAG/Rij rat model of generalized non-convulsive, absence-like epilepsy[45]. For this purpose **31c**, the first pyridine containing scaffold in our hands, was selected as a lead candidate. Beside showing improved HLM stability, **31c** also displayed suitable solubility (solubility at pH 7 = 42 μg/mL, solubility FaSSIF = 89 μg/mL, and solubility FeSSIF = 318 μg/mL). As this derivative was shown to be unstable in RLM, we performed a pharmacokinetic experiment in Wistar rats at a high dose of 100 mg/kg *p.o.*, aiming at saturation of the metabolism *in vivo* (Table 8). At this dose, **31c** showed high exposure in plasma with a C_{max} of 5440 ng/mL and a AUC of 21800 (ng*h/mL)[46]. Penetration of the blood brain barrier was studied at the same dose 1 h after oral administration. The results are

summarized in Table 9. The compound was only moderately penetrating the BBB as shown by a total [B]/[P] ratio of only 24% and an unbound [B]u/[P]u ratio of only 27%. However, using a brain free fraction of 0.022, a free concentration of 35 nM in the brain was calculated, which corresponds to roughly 0.25 times, 0.15 times and 1.5 times the IC_{50} on the human recombinant $Ca_v3.1$, $Ca_v3.2$ and $Ca_v3.3$ channels respectively. Despite the relatively low brain exposure and the modest activity on the Cav3.1 and Cav3.2 T-type calcium channels, derivative **31c** was selected for assessing its *in vivo* efficacy in the WAG/Rij rat model of generalized non-convulsive absence-like epilepsy. To increase the possibility of *in vivo* efficacy, the two enantiomers of **31c** were separated by preparative chiral HPLC. Active derivative **(3*R*,5*S*)-31c** showed an improved potency of approximately 2.3 times on Cav3.2 channels and 2 times on Cav3.3 channels compared to **31c** and also the stability in human liver microsomes showed to be improved compared to the racemic mixture (Figure 5). Male WAG/Rij rats older than 6 months were implanted with telemetric transmitters allowing continuous recording of the electroencephalogram and were administered with a single oral dose of 100 mg/kg **(3*R*,5*S*)-31c** (or matching vehicle) at the beginning of their nocturnal active phase (Figure 6). At this dose **(3*R*,5*S*)-31c** decreased the number of seizures by 50% over the 12h night period following administration compared to vehicle (**(3*R*,5*S*)-31c**: 153 ± 21, vehicle: 307 ± 31, p = 0.0005, paired t-test, Fig. 6b) including 3 hours of full seizure suppression (Fig. 6a). As a consequence, the cumulated duration of seizures was also reduced (-50% compared to vehicle; **(3*R*,5*S*)-31c**: 662 ± 120, vehicle: 1330 ± 192, p = 0.0017, paired t-test, Fig. 6c). Moreover, at this dose, the compound was well tolerated. The outcome of this experiment underlines the potential of the 1,4-benzodiazepine class for reduction of generalized non-convulsive seizures in the WAG/Rij rat model of absence-like epilepsy. In addition, whereas *in vivo* efficacy on models of absence-

like epilepsy was reported with triple T-type calcium channels[17, 18], data generated with **(3*R*,5*S*)-31c,** which is 10 times more potent on $Ca_v3.3$ channels compared to $Ca_v3.1$ or $Ca_v3.2$ channels, suggest that the $Ca_v3.3$ T-type channel might play a significant role in this context. The relative implication of the different T-type calcium channel subtypes in epilepsy would need selective compound for one or the other T-type calcium channel subtypes.

Table 8: Pharmacokinetic Data for Compound 31c

Route	Species	Dose (mg/kg)	Cmax (ng/mL)	Tmax (h)	AUC (ng*h/mL)
Oral	Rat[b]	100[c]	5440	0.5	21800

[a] Data represent means (n=2). [b]male (Wistar) [c] Suspension in MC 0.5%, pH 4.38.

Table 9: Concentrations in plasma, CSF and brain tissue in the rat for Compound 31c[a], 1h after oral dosing (100 mg/kg[b]).

Total brain concentration (nM)	Total plasma concentration (nM)	[B]/[P] Ratio	Unbound brain concentration (nM)[c]	Unbound plasma concentration (nM)[d]	[B]u/[P]u Ratio	CSF Concentration [nM]
1596 ± 453	6783 ± 998	24%	35 ± 10	128 ± 19	27%	494 ± 414

[a] Data represent means ± SD (n=3) [b] 10% PEG400 / 90% MC0.5% [c] fu,brain 0.022; [d] fu,plasma 0.019.

Figure 5. Activities of the Enantiomers of 31c

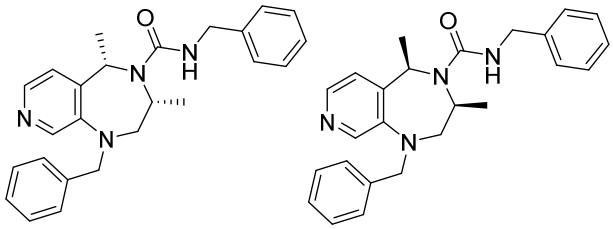

(3*R*,5*S*)-31c

Ca_v 3.1 IC_{50} = 138 ± 5 nM (n=3)
Ca_v 3.2 IC_{50} = 102 ± 36 nM (n=3)
Ca_v 3.3 IC_{50}= 11 ± 1 nM (n=3)

HLM (µL/min/mg)= 56 (n=1)
RLM (µL/min/mg)= 1156 (n=1)

(3*S*,5*R*)-31c

Ca_v 3.1 IC_{50} = > 10000 nM (n=3)
Ca_v 3.2 IC_{50} = > 11000 nM (n=3)
Ca_v 3.3 IC_{50} = > 10000 nM (n=3)

Figure 6. Effect of (3*R*, 5*S*)-31c on number (a, b) and cumulated duration (c) of seizures in telemetered male WAG/Rij rats. Rats (older than 6 months) were administered a single oral dose of vehicle (10% PEG400 / 90% MC0.5%) or 100 mg/kg **(3*R*, 5*S*)-31c** (arrow) just before the beginning of the dark phase (grey zones). Data are expressed per hour (a) or in12-h periods (b, c) as mean ± standard error of the mean (SEM) (n=7 per group). Paired t-test: *** $p<0.001$, ** $p<0.01$ vs. vehicle.

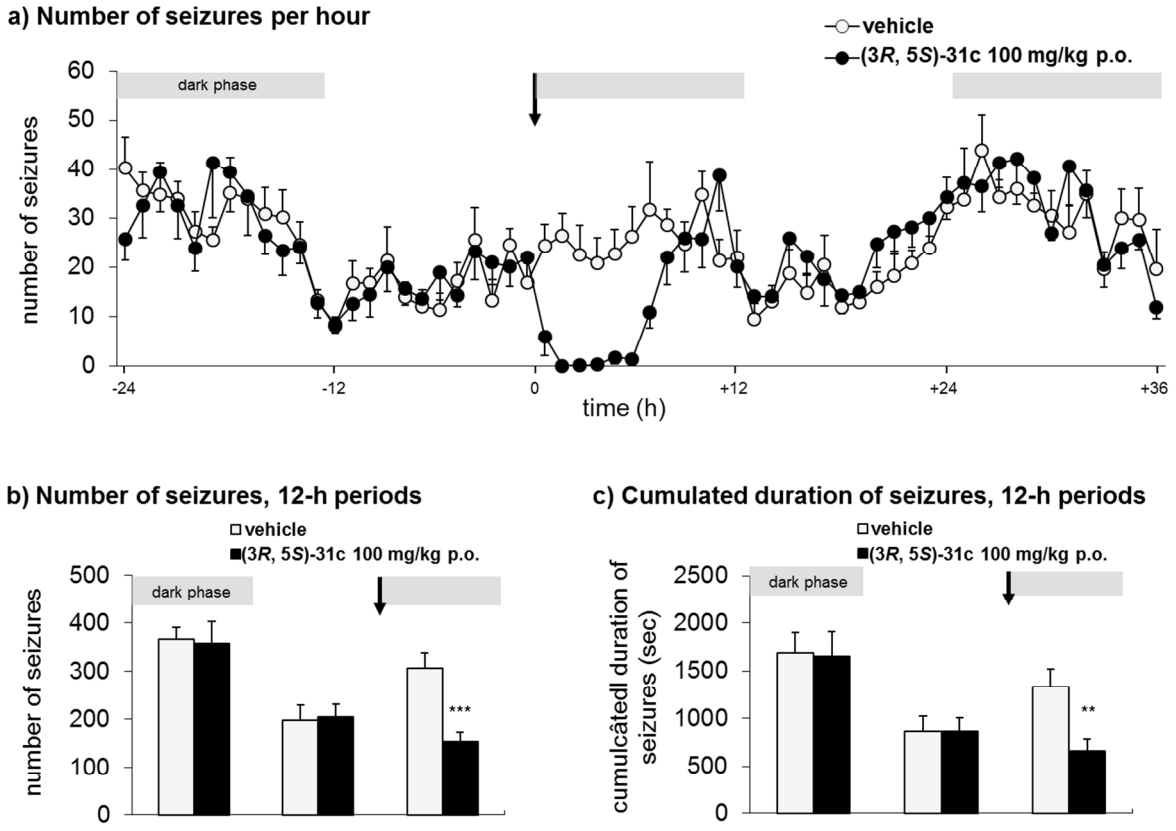

CONCLUSION

We have described here a Hit to Lead work which led to the discovery of the new triple T-type calcium channel blocker **(3*R*, 5*S*)-31c**. Starting from HTS hit **4** with poor physicochemical and *in vitro* DMPK properties, we were able to establish a clear SAR and to identify moieties allowing for the improvement of the physicochemical properties of the molecule. Incorporating a *N* atom to the central benzodiazipinic scaffold at 8-position allowed to improve the HLM stability. Introduction of fluorine atom in position 6 of the benzodiazepine or pyridodiazepine scaffold allowed to stabilize the molecules metabolically. Additionally, the addition of a fluorine atom on the pyridodiazepine decreased the pKa and concomitantly lowered the MDR1 efflux ratio. SAR studies with this scaffold led to the discovery of potent pyridodiazepines. Compound **31c** was the first in the pyridine sub series showing interesting HLM stability and was selected

for *in vivo* efficacy studies. Even with a rather low brain penetration and a modest activity on $Ca_v3.1$ and 3.2 T-type channels, **(3*R*, 5*S*)-31c** showed strong efficacy in the WAG/Rij rat model underlining the importance of $Ca_v3.3$ T-type calcium channel subtype in the pathophysiology of generalized non-convulsive absence-like epilepsy.

EXPERIMENTAL SECTION

Chemistry. All reagents and solvents were used as purchased from commercial sources. Moisture sensitive reactions were carried out under a nitrogen atmosphere. ^{1}H-NMR spectra were recorded at rt with a *Brucker NMR 500* spectrometer ^{1}H (500 MHz) equipped with a Bruker's DCH cryoprobe. Chemical shifts are reported in ppm downfield from tetramethylsilane using residual solvent signals as internal reference. The multiplicity is described as singulet s, doublet d, triplet t, quadruplet q, quintuplet quint, hextet h, heptuplet hept, multiplet m, apparent app. Broad signals are indicated as br. Final compounds were purified to ≥95% purity as assessed by analytical liquid chromatography with the following method: LC-MS conditions 01: Analytical. Pump: Agilent G4220A, MS: Thermo MSQ Plus, DAD: Agilent G4220A, ELSD: Sedere Sedex 90. Column: Zorbax SB-AQ 3.5 μm, 4.6x50 mm ID from Agilent Technologies, thermostated in the Dionex TCC-3200 compartment. Eluents: A: H_2O + 0.04% TFA; B: CH_3CN. Eluent MakeUp: CH_3CN / H_2O 7:3 at 0.250 mL/min. Method: Gradient: 5% B → 95% B over 1.07 min. Flow: 4.5 mL/min. Detection: UV/Vis and/or ELSD, and MS, t_R is given in min. LC-MS conditions 02: Analytical. Pump: Agilent G4220A, MS: Thermo MSQ Plus, DAD: Agilent G4212A. Column: Waters BEH C18, 3.0x50mm, 2.5um, Eluents: A: water/NH_3 [(NH_3)]= 13 mmol/L; B: CH_3CN. Eluent MakeUp: Buffer, [NH_4HCOO] = 10 mmol/L. Method: Gradient: 5% B → 95% B over 1.20 min. Flow: 1.6 mL/min. Detection: UV/Vis and MS, t_R is given in min. LC-chiral analytical: Column: Chiralpack AD-H 250x4.6mm ID, 5um. Eluents: A: 10.0%

heptane 0.05% DEA; B: 90.0% Ethanol 0.05% DEA. Flow: 0.800 mL/min. Detection: UV 210 nm.

(±)-tert-*Butyl-(1-((4-cyanopyridin-3-yl)amino)propan-2-yl)carbamate (**28**)*. A mixture of 3-fluoro-4-cyano-pyridine (2.42 mL, 23.8 mmol, 1 eq.), (±)-*tert*-butyl (1-aminopropan-2-yl) carbamate (4.57 mg, 26.20 mmol, 1.1 eq.) and triethylamine (9.9 mL, 71.5 mmol, 3 eq.) in NMP (25 mL) was stirred at 90 °C overnight. Once at rt, water was added to the reaction mixture. The precipitate was filtered, washed with water. The solid was dissolved in DCM and washed once again with water. The organic layer was separated, dried over $MgSO_4$, filtered and the solvent removed under reduced pressure to give **28** (5.58 g, 85%) as an off-white solid. The compound was used as such without further purification. LC-MS-conditions 01: t_R = 0.69 min, $[M+H]^+$ = 277.24. ^{1}H NMR (500 MHz, $CDCl_3$) δ: 8.21-8.28 (m, 1 H), 8.00 (d, J = 4.9 Hz, 1 H), 7.30 (d, J = 5.0 Hz, 1 H), 5.68 (br s, 1 H), 4.53-4.61 (m, 1 H), 4.01-4.15 (m, 1 H), 3.39-3.45 (m, 1 H), 3.19-3.31 (m, 1 H), 1.48 (s, 9 H), 1.30 (d, J = 6.8 Hz, 3 H).

(±)-tert-*Butyl-(1-((4-acetylpyridin-3-yl)amino)propan-2-yl)carbamate*. A flame-dried round bottom double neck flask under N_2 atmosphere was charged with a solution of **28** (5.58 g, 20.2 mmol, 1 eq.) in dry Et_2O (70 mL) and cooled to -78 °C. Methyllithium (1.6M in Et_2O, 63.1 mL, 101 mmol, 5 eq.) was added dropwise at -78 °C and the solution was allowed to stir at 0 °C during 7 h. The solution was cooled to -78 °C and methyllithium (1.6M in Et_2O, 12.6 mL, 20.2 mmol, 1 eq.) was added to the reaction mixture again. After stirring at 0 °C during 5 h, 2 N aq. HCl soln. was carefully added and the mixture was stirred for 30 min until complete hydrolysis was observed. The biphasic mixture was adjusted to pH 10-11 with 5% aq. soln. NaOH and extracted with EtOAc. The organic layer was washed with brine, dried over $MgSO_4$, filtered and concentrated under reduced pressure. The crude was purified by Flashmaster (heptane to

heptane/EtOAc 1:1) to give (±)-*tert*-butyl-(1-((4-acetylpyridin-3-yl)amino)propan-2-yl)carbamate (3.090 g, 52%). Rf (heptane/EtOAc 4:6) = 0.32. LC-MS-conditions 01: t_R = 0.60 min, $[M+H]^+$ = 294.25. ^{1}H NMR (500 MHz, $CDCl_3$) δ: 8.64 (s, 1 H), 8.41 (s, 1 H), 7.97 (d, J = 5.2 Hz, 1 H), 7.50 (d, J = 5.2 Hz, 1 H), 4.44-4.56 (m, 1 H), 3.96-4.05 (m, 1 H), 3.34-3.46 (m, 2 H), 2.63 (s, 3 H), 1.47 (s, 9 H), 1.27 (d, J = 6.8 Hz, 3 H).

*(±)-3,5-Dimethyl-2,3-dihydro-1*H*-pyrido[3,4-e][1,4]diazepine (**29**)*. To a solution of (±)-*tert*-butyl-(1-((4-acetylpyridin-3-yl)amino)propan-2-yl)carbamate (3.09 g, 10.5 mmol, 1 eq.) in dioxane (7 mL) was added 4M HCl in dioxane (10.5 mL, 42 mmol, 4 eq.) and the solution was stirred at rt overnight until the Boc deprotection was complete. The solvents were partially concentrated under reduced pressure, and the crude mixture purified by catch and release protocol (SCX, Biotage) to give **29** (1.872 g, 100%) as yellow oil. The compound was used as such without further purification. LC-MS-conditions 01: t_R = 0.35 min, $[M+H]^+$ = 176.38. ^{1}H NMR (500 MHz, DMSO) δ: 8.04 (s, 1 H), 7.72 (d, J = 5.3 Hz, 1 H), 7.21 (d, J = 5.3 Hz, 1 H), 6.56 (app d, J = 6.0 Hz, 1 H), 3.56-3.63 (m, 1 H), 3.38 (ddd, J = 1.5, 6.7, 12.2 Hz, 1 H), 3.23 (ddd, J = 2.1, 7.8, 12.2 Hz, 1 H), 2.31 (d, J = 1.2 Hz, 3 H), 1.29 (d, J = 6.7 Hz, 3 H).

*(±)-1-Benzyl-3,5-dimethyl-2,3-dihydro-1*H*-pyrido[3,4-e][1,4]diazepine*. In a round bottom double neck flask under a N_2 atmosphere, NaH (60% dispersion in mineral oil, 1.26 g, 31.6 mmol, 1.4 eq.) was added at 0 °C to a stirred solution of **29** (3.95 g, 22.5 mmol, 1 eq.) in DMF (121 mL). After 20min stirring at 0 °C, benzyl bromide (3.21 mL, 27 mmol, 1.2 eq.) was added and the mixture was then stirred at 70 °C for 2h. The reaction mixture was cooled to 0 °C and carefully quenched with 2N aq. HCl. and washed with EtOAc. The aq. layer was adjusted to pH 10-11 with 1N aq. NaOH soln. and extracted again with EtOAc. The combined organic layers were dried over $MgSO_4$, filtered and concentrated under reduced pressure. The residue was

purified Flashmaster (heptane to heptane/EtOAc (10% Et_3N) 8:2) to give (±)-1-benzyl-3,5-dimethyl-2,3-dihydro-1H-pyrido[3,4-e][1,4]diazepine (3.60 g, 60%) as a yellow oil. R_f (silica KP_NH, heptane/EtOAc 7:3) = 0.30. LC-MS-conditions 01: t_R= 0.55 min, $[M+H]^+$ = 266.26. ^1H NMR (500 MHz, $CDCl_3$) δ: 8.28 (s, 1 H), 8.21 (d, J = 4.9 Hz, 1 H), 7.33-7.37 (m, 2 H), 7.26-7.28 (m, 3 H), 7.11 (d, J = 4.8 Hz, 1 H), 4.58 (d, J = 14.9 Hz, 1 H), 4.24 (d, J = 14.9 Hz, 1 H), 3.65-3.70 (m, 1 H), 3.57 (t, J = 10.8 Hz, 1 H), 3.23 (dd, J = 3.0, 10.8 Hz, 1 H), 2.43 (br s, 3 H), 1.32 (d, J = 6.4 Hz, 3 H).

*(±)-1-Benzyl-3,5-*cis*-dimethyl-2,3,4,5-tetrahydro-1*H*-pyrido[3,4-e][1,4]diazepine (**cis-*30*).* A solution of (±)-1-benzyl-3,5-dimethyl-2,3-dihydro-1H-pyrido[3,4-e][1,4]diazepine (3.60 g, 13.6 mmol, 1 eq.) in MeOH (120 mL) was stirred at rt under an H_2 atmosphere (baloon) in presence of Pd/C (1.93 mg, 0.906 mmol, 0.07 eq.) as catalyst for 1h30min. The mixture was filtered over celite and the solvent removed under reduced pressure. The residue was purified by Flashmaster (heptane to heptane/EtOAc (10% NEt_3) 8:2) to give ***cis*-30** (2.81 g, 77%) as a yellow oil. LC-MS-conditions 02: t_R = 0.87 min, $[M+H]^+$ = 268.17. ^1H NMR (500 MHz, DMSO) δ: 8.26 (s, 1 H), 8.13 (d, J = 4.9 Hz, 1 H), 7.42 (app d, J = 7.1 Hz, 2 H), 7.32-7.35 (tt, J = 1.5, 7.4 Hz, 2 H), 7.24 (tt, J = 1.2, 7.4, 1 H), 7.16 (d, J = 4.9 Hz, 1 H), 4.60 (d, J = 14.3 Hz, 1 H), 4.30 (d, J = 14.3 Hz, 1 H), 3.92 (q, J = 6.8 Hz, 1 H), 3.05 (dd, J = 2.7, 13.0 Hz, 1 H), 2.89-2.98 (m, 1 H), 2.18 (dd, J = 9.8, 13.1 Hz, 1 H), 1.81 (br s, 1 H), 1.45 (d, J = 6.8 Hz, 3 H), 0.80 (d, J = 6.4 Hz, 3 H).

*(±)-*N*,1-Dibenzyl-3,5-*cis*-dimethyl-1,2,3,5-tetrahydro-4*H*-pyrido[3,4-e][1,4]diazepine-4-carboxamide* (***31c***). To a solution of ***cis*-30** (20 mg, 0.0748 mmol, 1 eq.) in DCM (0.5 mL), benzyl isocyanate (0.010 mL, 0.082 mmol, 1.1 eq.) and DIPEA (0.0384 mL, 0.224 mmol, 3 eq.) were added. The mixture was stirred at rt for 18h. The reaction mixture was concentrated in vacuo and the residue was purified by Flashmaster (heptane to heptane/EtOAc 3:7) to yield **31c**

(24 mg, 80%) as a white solid. Rf silica (heptane/EtOAc 3:7) = 0.35. LC-MS-conditions 01: t_R = 0.69min, $[M+H]^+$ = 401.11. ^{1}H NMR (500 MHz, DMSO) δ: 7.81 (d, J = 4.1 Hz, 2 H), 7.19-7.31 (m, 10 H), 7.06 (t, J = 5.7 Hz, 1 H), 7.03 (d, J = 5.0 Hz, 1 H), 5.80-5.90 (m, 1 H), 4.71 (d, J= 16.7 Hz, 1 H), 4.58 (d, J= 16.7 Hz, 1 H), 4.36-4.39 (m, 1 H), 4.31 (dd, J = 5.8, 15.5 Hz, 1 H), 4.26 (dd, J = 5.8, 15.5 Hz, 1 H), 3.77 (dd, J = 11.8, 15.3 Hz, 1 H), 3.38-3.43 (m, 1 H), 1.70 (d, J = 7.6 Hz, 3 H), 1.19 (d, J = 6.6 Hz, 3 H).

*(3*R*,5*S*)*-N*,1-Dibenzyl-3,5-dimethyl-1,2,3,5-tetrahydro-4*H*-pyrido[3,4-e][1,4]diazepine-4-carboxamide ((**3**R,5S)-31c)* and *(3*S*,5*R*)*-N*,1-dibenzyl-3,5-dimethyl-1,2,3,5-tetrahydro-4*H*-pyrido[3,4-e][1,4]diazepine-4-carboxamide ((**3**S,5R)-31c)*. (±)-*N*,1-dibenzyl-3,5-*cis*-dimethyl-1,2,3,5-tetrahydro-4*H*-pyrido[3,4-e][1,4]diazepine-4-carboxamide **31c** (986 mg, 2.59 mmol) was separated by chiral preparative HPLC (ChiralPak AD-H, 30x250mm, 5um; heptane/EtOH 0.1% DEA 1:2; Flow 34 mL/min) to give **(3*R*,5*S*)-31c** (480 mg, 48%) and **(3*S*,5*R*)-31c** (485 mg, 49%) as white solids. **(3*R*,5*S*)-31c**: LC chiral analytical: t_R= 6.8min. **(3*R*,5*S*)-31c**: LC chiral analytical: t_R= 4.63 min.

Biology. Measurement of calcium T-channel flux by means of FLIPR assay: HEK293 cells recombinantly expressing the voltage-dependent T-type calcium channel subunit alpha-1G ($Ca_v3.1$) or the subunit alpha-1H ($Ca_v3.2$) or the subunit alpha-1I ($Ca_v3.3$) were assayed for calcium flux using the calcium indicator dye Fluo-4-AM (Molecular Devices) and FLIPR technology (Fluorometric Imaging Plate Reader, Molecular Devices). HEK293 cells recombinantly expressing $Ca_v3.1$, $Ca_v3.2$ or $Ca_v3.3$ were maintained in DMEM growth medium (Life Technologies) supplemented with 10 % Fetal Bovine Serum (FBS), 100 U/ml penicillin (Life Technologies), 100 μg/ml streptomycin (Life Technologies) and 1 mg/ml G418 (Life Technologies). Cells were seeded into PureCoat Amine coated 384-well black, clear bottom

plates (BD Biosciences) at a density of 30,000 cells/well and plates were incubated overnight at 37 °C. Immediately prior to performing the assay, medium was removed and cells were treated for 1 hour at 37 °C with dye loading buffer containing HBSS 1X (137 mM NaCl; 5.4 mM KCl; 0.25 mM Na_2HPO_4; 1.3 mM $CaCl_2$; 0.4 mM $MgSO_4$; 0.5 mM $MgCl_2$; 0.4 mM KH_2PO_4, pH 7.4), 0.375 g/L $NaHCO_3$, 20 mM Hepes, supplemented with 3 μM Fluo-4-AM and 0.15 % Pluronic (Life Technologies). The cells were then washed three times with assay buffer (HBSS 1X; 0.375 g/L $NaHCO_3$; 20 mM Hepes; 1 % FBS; pH 7.4) and allowed to rest in 50 μl of wash buffer for 30 minutes.

Stock solutions of test compounds were prepared to a concentration of 10 mM in DMSO. Serial dilutions of the compounds were prepared in TEAC buffer (100 mM tetraethylammonium chloride; 20 mM Hepes; 2.5 mM $CaCl_2$; 5 mM KCl; 1 mM $MgCl_2$; 1 % FBS; pH 7.2). Test compounds were added to the cells to give a 3-fold dilution range from 10 μM to 0.05 nM. The compounds were incubated with the cells for 3 minutes and Ca^{2+} entry was stimulated by adding $CaCl_2$ to a final concentration of 10 mM. The kinetics of fluorescence increase were recorded for every well and the area under the fluorescence trace for every compound concentration was used to generate inhibition curves using non-linear regression sigmoidal concentration-response curve analysis with in-house software. IC_{50} values were calculated and represent the compound concentration required to inhibit 50% of the signal that is obtained in the presence of vehicle instead of test compound.

Metabolic Stability in liver Microsomes. Liver microsomal preparations from humans (pool of 48 donors) and male Wistar rat (pool of 4 animals) were purchased from Becton Dickinson (Basel, Switzerland). They were employed at a microsomal protein concentration of 0.5 mg/mL in the presence of a NADPH-regenerating system. Incubations of compounds were performed at

a single concentration of 1 μM at 37°C. The reaction was initiated by addition of the NADPH-regenerating system and terminated after appropriate time periods up to 15 min by addition of ice-cold methanol. After centrifugation, samples were analysed by LC-MS-MS. Intrinsic clearances were determined by initial first order disappearance rates. The total concentration of DMSO in the assay did not exceed 0.1 %.

Unbound fraction. The fraction unbound in plasma and in brain was determined using RED (rapid equilibrium dialysis) plates from Thermo Scientific (Rockford, lL, USA). Samples were analysed by LC-MS/MS.

Pharmacological protocol. Male Wistar rats and WAG/Rij rats were purchased from Harlan (Horst Netherlands) and Charles River (Sulzfeld, Germany) respectively. All animals were maintained under standard lab conditions (temperature 20 ± 2°C, relative humidity 55–70%, on a 12 h light / 12 h dark cycle from 6 am to 6 pm) with free access to normal chow and water. The experimental procedures used in this study were approved based on international guidelines and adherence to Swiss federal regulations on animal experimentation (license BL 205 for EEG experiments, BL 426 for the in vivo brain penetration potential experiment, and BL 169 for pharmacokinetic studies).

In vivo brain penetration potential evaluation

In order to assess brain penetration, concentrations of the compound were measured in plasma, cerebrospinal fluid (CSF) and brain sampled following administration to male Wistar rats (the background strain of the WAG/Rij rats). Sampling was done 1 h after dosing, allowing equilibrium between plasma and brain drug concentration. Rats were treated orally with a dose of 100 mg/kg formulated in 10% polyethylene glycol 400 / 90% methylcelluloce 0.5%, aqueous solution) and sacrificed 1 h later by an overdose of CO_2. Blood was sampled from the vena cava

caudalis into plastic tubes coated with EDTA (ethylenediamine tetraacetic acid) as anticoagulant and centrifuged to yield plasma. CSF was sampled from the cisterna magma with careful attention to avoid blood contamination. Brain was sampled after cardiac perfusion of 10 mL NaCl 0.9% and homogenized into one volume of cold phosphate buffer (pH 7.4). Following extraction with methanol, concentrations of the compound in plasma, CSF and brain are determined using liquid chromatography coupled to mass spectrometry.

WAG/Rij rat model

Surgery: Adult male WAG/Rij rats (aged at least 6 months, body weight 300-350g) were equipped with the TL11M2-F20-EET implant (Data Science International, St Paul, MN, USA) that consists of 4 leads (2 pairs) for EEG and electromyographic (EMG) measurements by telemetry. For surgery, rats were anesthetized with isoflurane and placed in a stereotaxic apparatus. The transmitter's body was placed subcutaneously along the dorsal flank of the rat and EEG and EMG leads were routed subcutaneously to an incision accessing the cranium. Trepanations were made in the skull and EEG electrodes were placed on the surface of the cortex (from bregma: 1st electrode: AP: -1mm, ML: -2.5mm, DV: 0mm; from lambda: 2nd electrode: AP: +1mm, ML: -3.5mm, DV: 0mm) and secured to the skull with screws and dental acrylate. The EMG leads were placed in either side of cervical muscles and sutured in place. After one week of recovery, rats could be included in pharmacology studies.

Procedure: The entire telemetry system originates from Data Sciences International (USA). It comprises transmitters, receiver plates (PhysioTel RPC-1), data exchange matrixes (1 for 4 receivers) and computers installed with the Dataquest A.R.T. 4.1 Gold software for data acquisition (1 computer for 8 receivers). For continuous EEG/EMG recordings, single-housed implanted rats, in their home cage, were placed on the receiver plate within a sound attenuating

scantainer that is equipped with light and fan to ensure a quiet environment. EEG seizures were evaluated using Neuroscore 2.0 or 2.1 software (Data Science International, St Paul, MN, USA).

Drug testing: Acute drug effects on spontaneous seizures were evaluated in groups of 6-8 rats in a randomized cross-over design with at least 72h between drug and vehicle applications. Following a 24-h baseline recording, drug or vehicle was administered 30 minutes before beginning of the dark phase and number and duration of EEG seizures were assessed andintegrated in 12-h periods. Statistical analysis was performed by paired t-test for effects of drug vs. vehicle within each 12-h period.

Pharmacokinetics in the Rat. Oral administration at a dose of 100 mg/kg was performed by gavage. For that, the compounds were formulated in an acidified 0.5% methylcellulose suspension. Serial blood samples of 0.25 mL each were taken pre-dose and at 30 min, 1, 2, 3, 4, 6, 8 and 24 h post-dose into vials containing EDTA as anticoagulant. All animals had free access to food and water during the entire duration of the experiments. Plasma samples were analyzed after protein precipitation with methanol and centrifugation at 3220 g for 20 min at 4 °C using liquid chromatography coupled to mass spectrometry (LC-MS-MS) using appropriate calibration curves and an internal standard (close analogue) and bioanalytical quality controls. Pharmacokinetic parameters were estimated with the Phoenix Winnonlin 6.3 software package (Pharsight) using non-compartmental analysis.

ACCESSION CODE

The corresponding data set has been deposited at the Cambridge Crystallographic Data Centre, 12 Union Road, Cambridge CB2 1EZ, United Kingdom, http://www.ccdc.cam. ac.uk/, under the following deposition number: 1492195 (compound **(3*S*,5*R*)-37**).

Corresponding Author

*Phone: +41 61 565 65 65; fax: +41 61 565 65 00; E-Mail: olivier.bezencon@actelion.com

Present Addresses

†Thomas Pfeifer: ADME & more, Märktweg 30, D-79576 Weil am Rhein, Germany.

Author Contributions

The manuscript was written through contributions of all authors. All authors have given approval to the final version of the manuscript. ‡These authors contributed equally.

Notes

The authors declare no competing financial interest.

ACKNOWLEDGMENT

The authors thank René Vogelsanger and Michael Erhardt for chiral analysis and separation; Sylvia Richard, Siefke Siefken, and Lise-May Viment for the preparation of focused libraries; Daniel Bur for the X-ray analysis; Eileen Hubert, Hélène Roellinger, Hélène Massinet for their contribution in the pharmacological studies; Aude Weigel for the PK study; Michel Rauser and Rolf Wuest for DMPK studies; and Thomas Weller for his continuous support.

ABBREVIATIONS

AUC, area under the curve; BBB, blood-brain barrier; BTFFH, fluoro-*N*,*N*,*N'*,*N'*-bis(tetramethylene)formamidinium hexafluorophosphate; Boc, *tert*-butoxycarbonyl; Cl_{int}, intrinsic clearance; C_{max}, maximum concentration; Cmpd., compound; CSF, cerebrospinal fluid; DCE, 1,2-dichloroethane; DCM, dichloromethane; DEA, diethyl amine; DIPEA, *N*,*N*-diisopropylethylamine; DMAC, *N*,*N*-dimethylacetamide; DMF, dimethylformamide; DMPK,

drug metabolism and pharmacokinetics; DMS, dimethyl sulfide; DMSO, dimethyl sulfoxide; dppf, 1,1'-bis(diphenylphosphino)ferrocene; EDC•HCl, *N*-[3-(dimethylamino)prop-1-yl]-*N*'-ethylcarbodiimide hydrochloride; FaSSIF, fasted state simulated intestinal fluid; FeSSIF, fed state simulated intestinal fluid; HATU, 1-[bis(dimethylamino)methylene]-1H-1,2,3-triazolo[4,5-b]pyridinium 3-oxid hexafluorophosphate; HLM, human liver microsomes; M, molar (moles per liter); MC, methyl cellulose; MDR1, multidrug resistance protein 1; MeCN, acetonitrile; NEt_3, triethylamine; NMP, *N*-methyl-2-pyrrolidone; pd_2dba_3, tris(dibenzylideneacetone)dipalladium(0); PEG, polyethylene glycol; PK, pharmacokinetics; pKa, negative decadic logarithm of the ionization constant (K_a); PMHS, polymethylhydrosiloxane; RLM, rat liver microsomes; rt, room temperature; SAR, structure-activity relationship; THF, tetrahydrofuran; T_{max}, time of maximum concentration; TFA, trifluoroacetic acid.

REFERENCES

1. Remy, S.; Beck, H. Molecular and cellular mechanisms of pharmacoresistance in epilepsy. *Brain* **2006**, *129*, 18-35.

2. Franco, V.; French, J. A.; Perucca, E. Challenges in the clinical development of new antiepileptic drugs. *Pharmacol. Res.* **2016**, *103*, 95-104.

3. (a) Loscher, W.; Klitgaard, H.; Twyman, R. E.; Schmidt, D. New avenues for anti-epileptic drug discovery and development. *Nat. Rev. Drug Discovery* **2013**, *12*, 757-776. (b) French, J. A.; White, H. S.; Klitgaard, H.; Holmes, G. L.; Privitera, M. D.; Cole, A. J.; Quay, E.; Wiebe, S.; Schmidt, D.; Porter, R. J.; Arzimanoglou, A.; Trinka, E.; Perucca, E. Development of new treatment approaches for epilepsy: unmet needs and opportunities. *Epilepsia* **2013**, *54 Suppl 4*, 3-12.

4. Perez-Reyes, E. Molecular physiology of low-voltage-activated t-type calcium channels. *Physiol. Rev.* **2003**, *83*, 117-161.

5. Talley, E. M.; Cribbs, L. L.; Lee, J. H.; Daud, A.; Perez-Reyes, E.; Bayliss, D. A. Differential distribution of three members of a gene family encoding low voltage-activated (T-type) calcium channels. *J. Neurosci.* **1999**, *19*, 1895-1911.

6. Cheong, E.; Shin, H. S. T-type Ca^{2+} channels in normal and abnormal brain functions. *Physiol. Rev.* **2013**, *93*, 961-992.

7. Lambert, R. C.; Bessaih, T.; Crunelli, V.; Leresche, N. The many faces of T-type calcium channels. *Pfluegers Arch.* **2014**, *466*, 415-423.

8. Shin, H. S.; Cheong, E. J.; Choi, S.; Lee, J.; Na, H. S. T-type Ca^{2+} channels as therapeutic targets in the nervous system. *Curr. Opin. Pharmacol.* **2008**, *8*, 33-41.

9. Yang, Y. C.; Tai, C. H.; Pan, M. K.; Kuo, C. C. The T-type calcium channel as a new therapeutic target for Parkinson's disease. *Pfluegers Arch.* **2014**, *466*, 747-755.

10. Francois, A.; Laffray, S.; Pizzoccaro, A.; Eschalier, A.; Bourinet, E. T-type calcium channels in chronic pain: mouse models and specific blockers. *Pfluegers Arch.* **2014**, *466*, 707-717.

11. Valerie, N. C.; Dziegielewska, B.; Hosing, A. S.; Augustin, E.; Gray, L. S.; Brautigan, D. L.; Larner, J. M.; Dziegielewski, J. Inhibition of T-type calcium channels disrupts Akt signaling and promotes apoptosis in glioblastoma cells. *Biochem. Pharmacol.* **2013**, *85*, 888-897.

12. Yang, Z. Q.; Schlegel, K. A.; Shu, Y.; Reger, T. S.; Cube, R.; Mattern, C.; Coleman, P. J.; Small, J.; Hartman, G. D.; Ballard, J.; Tang, C.; Kuo, Y.; Prueksaritanont, T.; Nuss, C. E.; Doran, S.; Fox, S. V.; Garson, S. L.; Li, Y.; Kraus, R. L.; Uebele, V. N.; Taylor, A. B.; Zeng, W.; Fang, W.; Chavez-Eng, C.; Troyer, M. D.; Luk, J. A.; Laethem, T.; Cook, W. O.; Renger, J.

J.; Barrow, J. C. Short-acting T-type calcium channel antagonists significantly modify sleep architecture in rodents. *ACS Med. Chem. Lett.* **2010**, *1*, 504-509.

13. Powell, K. L.; Cain, S. M.; Snutch, T. P.; O'Brien, T. J. Low threshold T-type calcium channels as targets for novel epilepsy treatments. *Br. J. Clin. Pharmacol.* **2014**, *77*, 729-739.

14. Zamponi, G. W.; Lory, P.; Perez-Reyes, E. Role of voltage-gated calcium channels in epilepsy. *Pfluegers Arch.* **2010**, *460*, 395-403.

15. Cheong, E.; Shin, H. S. T-type Ca^{2+} channels in absence epilepsy. *Pfluegers Arch.* **2014**, *466*, 719-734.

16. Kopecky, B. J.; Liang, R.; Bao, J. T-type calcium channel blockers as neuroprotective agents. *Pfluegers Arch.* **2014**, *466*, 757-765.

17. Yang, Z. Q.; Barrow, J. C.; Shipe, W. D.; Schlegel, K. A.; Shu, Y.; Yang, F. V.; Lindsley, C. W.; Rittle, K. E.; Bock, M. G.; Hartman, G. D.; Uebele, V. N.; Nuss, C. E.; Fox, S. V.; Kraus, R. L.; Doran, S. M.; Connolly, T. M.; Tang, C.; Ballard, J. E.; Kuo, Y.; Adarayan, E. D.; Prueksaritanont, T.; Zrada, M. M.; Marino, M. J.; Graufelds, V. K.; DiLella, A. G.; Reynolds, I. J.; Vargas, H. M.; Bunting, P. B.; Woltmann, R. F.; Magee, M. M.; Koblan, K. S.; Renger, J. J. Discovery of 1,4-substituted piperidines as potent and selective inhibitors of T-type calcium channels. *J. Med. Chem.* **2008**, *51*, 6471-6477.

18. Tringham, E.; Powell, K. L.; Cain, S. M.; Kuplast, K.; Mezeyova, J.; Weerapura, M.; Eduljee, C.; Jiang, X.; Smith, P.; Morrison, J. L.; Jones, N. C.; Braine, E.; Rind, G.; Fee-Maki, M.; Parker, D.; Pajouhesh, H.; Parmar, M.; O'Brien, T. J.; Snutch, T. P. T-type calcium channel blockers that attenuate thalamic burst firing and suppress absence seizures. *Sci. Transl. Med.* **2012**, *4*, 121ra119.

19. Ernst, W. L.; Zhang, Y.; Yoo, J. W.; Ernst, S. J.; Noebels, J. L. Genetic enhancement of thalamocortical network activity by elevating alpha 1g-mediated low-voltage-activated calcium current induces pure absence epilepsy. *J. Neurosci.* **2009**, *29*, 1615-1625.

20. Kim, D.; Song, I.; Keum, S.; Lee, T.; Jeong, M. J.; Kim, S. S.; McEnery, M. W.; Shin, H. S. Lack of the burst firing of thalamocortical relay neurons and resistance to absence seizures in mice lacking alpha(1G) T-type Ca(2+) channels. *Neuron* **2001**, *31*, 35-45.

21. Eckle, V. S.; Shcheglovitov, A.; Vitko, I.; Dey, D.; Yap, C. C.; Winckler, B.; Perez-Reyes, E. Mechanisms by which a CACNA1H mutation in epilepsy patients increases seizure susceptibility. *J. Physiol.* **2014**, *592*, 795-809.

22. Shipe, W. D.; Barrow, J. C.; Yang, Z. Q.; Lindsley, C. W.; Yang, F. V.; Schlegel, K. A.; Shu, Y.; Rittle, K. E.; Bock, M. G.; Hartman, G. D.; Tang, C.; Ballard, J. E.; Kuo, Y.; Adarayan, E. D.; Prueksaritanont, T.; Zrada, M. M.; Uebele, V. N.; Nuss, C. E.; Connolly, T. M.; Doran, S. M.; Fox, S. V.; Kraus, R. L.; Marino, M. J.; Graufelds, V. K.; Vargas, H. M.; Bunting, P. B.; Hasbun-Manning, M.; Evans, R. M.; Koblan, K. S.; Renger, J. J. Design, synthesis, and evaluation of a novel 4-aminomethyl-4-fluoropiperidine as a T-type Ca^{2+} channel antagonist. *J. Med. Chem.* **2008**, *51*, 3692-3695.

23. Giordanetto, F.; Knerr, L.; Wallberg, A. T-type calcium channels inhibitors: a patent review. *Expert Opin. Ther. Pat.* **2011**, *21*, 85-101.

24. Remen, L.; Bezencon, O.; Simons, L.; Gaston, R. D.; Downing, D.; Gatfield, J.; Roch, C.; Kessler, M.; Mosbacher, J.; Pfeifer, T.; Grisostomi, C.; Rey, M.; Ertel, E. A.; Moon, R. Preparation, antiepileptic activity and cardiovascular safety of dihydropyrazoles as brain-penetrant T-type calcium channel blockers. *J. Med. Chem.* **2016**, *59*, 8398-8411.

25. (a) Barrow J. C.; Bieber, K.-A. S.; Cube, R. V.; Mattern, M. C.; Reger, T. S.; Shu, Y.; Yang, Z.-Q. Pyridyl amide T-Type calcium channel antagonists. WO2007120729 A2, April 12, 2007. (b) Reger, T. S.; Yang, Z. Q.; Schlegel, K. A.; Shu, Y.; Mattern, C.; Cube, R.; Rittle, K. E.; McGaughey, G. B.; Hartman, G. D.; Tang, C.; Ballard, J.; Kuo, Y.; Prueksaritanont, T.; Nuss, C. E.; Doran, S. M.; Fox, S. V.; Garson, S. L.; Li, Y.; Kraus, R. L.; Uebele, V. N.; Renger, J. J.; Barrow, J. C. Pyridyl amides as potent inhibitors of T-type calcium channels. *Bioorg. Med. Chem. Lett.* **2011**, *21*, 1692-1696.

26. Egan, M. F.; Zhao, X.; Smith, A.; Troyer, M. D.; Uebele, V. N.; Pidkorytov, V.; Cox, K.; Murphy, M.; Snavely, D.; Lines, C.; Michelson, D. Randomized controlled study of the T-type calcium channel antagonist MK-8998 for the treatment of acute psychosis in patients with schizophrenia. *Hum. Psychopharmacol.* **2013**, *28*, 124-133.

27. Sakkaki, S.; Gangarossa, G.; Lerat, B.; Francon, D.; Forichon, L.; Chemin, J.; Valjent, E.; Lerner-Natoli, M.; Lory, P. Blockade of T-type calcium channels prevents tonic-clonic seizures in a maximal electroshock seizure model. *Neuropharmacology* **2015**, *101*, 320-329.

28. Zhang, Q.; Xia, Z.; Joshi, S.; Scott, V. E.; Jarvis, M. F. Optimization of ADME properties for sulfonamides leading to the discovery of a T-type calcium channel blocker, ABT-639. *ACS Med. Chem. Lett.* **2015**, *6*, 641-644.

29. Choi, K. H. The design and discovery of T-type calcium channel inhibitors for the treatment of central nervous system disorders. *Expert Opin. Drug Discovery* **2013**, *8*, 919-931.

30. Xie, X.; Van Deusen, A. L.; Vitko, I.; Babu, D. A.; Davies, L. A.; Huynh, N.; Cheng, H.; Yang, N.; Barrett, P. Q.; Perez-Reyes, E. Validation of high throughput screening assays against three subtypes of Ca(v)3 T-type channels using molecular and pharmacologic approaches. *Assay Drug Dev. Technol.* **2007**, *5*, 191-203.

31. Bogolubsky, A. V.; Moroz, Y. S.; Mykhailiuk, P. K.; Granat, D. S.; Pipko, S. E.; Konovets, A. I.; Doroschuk, R.; Tolmachev, A. Bis(2,2,2-trifluoroethyl) carbonate as a condensing agent in one-pot parallel synthesis of unsymmetrical aliphatic ureas. *ACS Comb. Sci.* **2014**, *16*, 303-308.

32. See supporting information for compound preparation.

33. Sorribes, I.; Junge, K.; Beller, M. Direct catalytic N-alkylation of amines with carboxylic acids. *J. Am. Chem. Soc.* **2014**, *136*, 14314-14319.

34. Carr, R. M.; Cable, K. M.; Wells, G. N.; Sutherland, D. R. A convenient method for the cyanation of aromatic iodo compounds. *J. Labelled Compd. Radiopharm.* **1994**, *34*, 887-897.

35. Rosenmund, K. W.; Struck, E. Das am Ringkohlenstoff gebundene Halogen und sein Ersatz durch andere Substituenten. I. Mitteilung: Ersatz des Halogens durch die Carboxylgruppe. *Ber. Dtsch. Chem. Ges. B* **1919**, *52*, 1749-1756.

36. von Braun, J.; Manz, G. Fluoranthen und seine Derivate. *Liebigs Ann. Chem.* **1931**, *488*, 111-126.

37. Connor, J. A.; Leeming, S. W.; Price, R. Influence of substrate structure on copper(I)-assisted cyanide substitution in aryl halides. *J. Chem. Soc., Perkin Trans.* **1990**, *1*, 1127-1132.

38. Pongratz, A. Untersuchungen über Perylen und seine Derivate. *Monatsh. Chem. Verw. Teile Anderer Wiss.* **1927**, *48*, 585-591.

39. Wang, Z. X.; Li, Y.; Guntoori, B. Novel process for the preparation of flecainide, its pharmaceutically acceptable salts and important intermediates thereof. US20050059825 A1, March 17, 2005.

40. Zhu, W.; Ma, D. Synthesis of aryl azides and vinyl azides *via* proline-promoted CuI-catalyzed coupling reactions. *Chem. Commun.* **2004**, 888-889.

41. Zhu, W.; Ma, D. Synthesis of aryl sulfones via L-proline-promoted CuI-catalyzed coupling reaction of aryl halides with sulfinic acid salts. *J. Org. Chem.* **2005**, *70*, 2696-2700.

42. Huang, Z.; Jin, J.; Machajewski, T. D.; Antonios-Mccrea, W. R.; Mckenna, M.; Poon, D.; Renhowe, P. A.; Sendzik, M.; Shafer, C. M.; Smith, A. Novel heterocyclic compounds and uses therof. WO2009115572 A2, September 24, 2009.

43. Zsebo, K. M.; Dahl, R. Methods for treating diseases associated with the modulation of serca. WO2010088450 A2, August 5, 2010.

44. Harbeson, S. L.; Tung, R. D. Deuterium in drug discovery and development. *Annu. Rep. Med. Chem.* **2011**, *46*, 403-417.

45. Coenen, A. M.; Van Luijtelaar, E. L. Genetic animal models for absence epilepsy: a review of the WAG/Rij strain of rats. *Behav. Genet.* **2003**, *33*, 635-655.

46. Another explanation for the high exposure observed could be due to autoinhibition of its clearance. (**3*R*,5*S*)-31c** showed an IC_{50} on CYP3A4 of 23-31 nM.

TOC

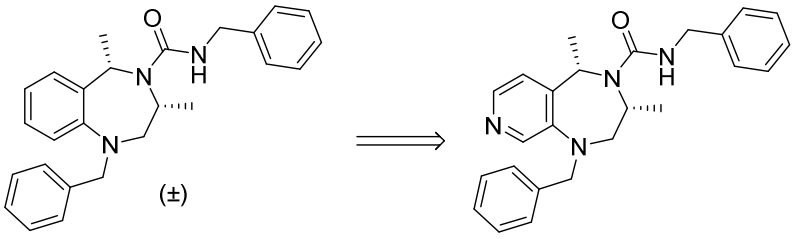

	4	**(3*R*, 5*S*)-31c**
$Ca_V3.1$ /3.2 /3.3 IC_{50} [nM]	17 ± 7 / 35 ± 25 / 8 ± 4	138 ± 5 / 102 ± 36 / 11 ± 1
Solubility [μg/mL] (pH=7/FaSSIF/FeSSIF)	<1 / 6 / 20	27 / 173 / >680
$logD_{7.4}$	>4.1	3.7
CL_{int} [μL/min/mg] (human/rat)	>1250 / >1250	56 / 1129